EFFECTS OF SURFACE CONTAMINATION ON XAS ANALYSIS OF DIAMOND-LIKE CARBON PREPARED BY HIGH POWER IMPULSE MAGNETRON SPUTTERING

Jidapa Lomon

A Thesis Submitted in Partial Fulfillment of the Requirements for the

Degree of Master of Science in Physics

Suranaree University of Technology

Academic Year 2018

ผลกระทบของพื้นผิวที่ปนเปื้อนต่อการวิเคราะห์ผลด้วยการดูดกลืนรังสีเอกซ์ของคาร์บอนคล้ายเพชรที่เตรียมโดยไฮพาวเวอร์อิมพัลส์แมกนีตรอนสปัตเตอริง

นางสาวจิดาภา ลมอ่อน

วิทยานิพนธ์นี้เป็นส่วนหนึ่งของการศึกษาตามหลักสูตรปริญญาวิทยาศาสตรมหาบัณฑิต
สาขาวิชาฟิสิกส์
มหาวิทยาลัยเทคโนโลยีสุรนารี
ปีการศึกษา 2561

EFFECTS OF SURFACE CONTAMINATION ON XAS ANALYSIS OF DIAMOND-LIKE CARBON PREPARED BY HIGH POWER IMPULSE MAGNETRON SPUTTERING

Suranaree University of Technology has approved this thesis submitted in partial fulfillment of the requirements for a Master's Degree.

Thesis Examining Committee

สิริโชค

(Asst. Prof. Dr. Sirichok Jungthawan)

Chairperson

Prayoon Song.

(Assoc. Prof. Dr. Prayoon Songsiriritthigul)

Member

(Asst. Prof. Dr. Phitsanu Poolcharuansin)

Member

(Dr. Hideki Nakajima)

Member

(Prof. Dr. Santi Maensiri)

Vice Rector Academic Affairs

and Internationalization

(Assoc. Prof. Dr. Worawat Meevasana)

Dean of Institute of Science

จิดาภา ลมอ่อน : ผลกระทบของพื้นผิวที่ปนเปื้อนต่อการวิเคราะห์ผลด้วยการดูดกลืนรังสีเอกซ์ของคาร์บอนคล้ายเพชรที่เตรียมโดยไฮพาวเวอร์อิมพัลส์แมกนีตรอนสปัตเตอริง (EFFECTS OF SURFACE CONTAMINATION ON XAS ANALYSIS OF DIAMOND-LIKE CARBON PREPARED BY HIGH POWER IMPULSE MAGNETRON SPUTTERING) อาจารย์ที่ปรึกษา : รองศาสตราจารย์ ดร.ประยูร ส่งสิริฤทธิกุล, 76 หน้า.

งานวิจัยนี้มุ่งเน้นการตรวจสอบผลกระทบของการปนเปื้อนของพื้นผิวต่อการตรวจวิเคราะห์ฟิล์มคาร์บอนคล้ายเพชร (DLC) โดยเทคนิคการดูดกลืนรังสีเอกซ์ (XAS) การปนเปื้อนดังกล่าวเกิดจากการสัมผัสกับอากาศในระหว่างการถ่ายโอนจากระบบเตรียมสารไปยังระบบวิเคราะห์ มันเป็นสิ่งที่หลีกเลี่ยงไม่ได้ที่พื้นผิวตัวอย่างจะถูกปนเปื้อนด้วยโมเลกุลของอากาศที่ถูกดูดซับ ในงานนี้ฟิล์ม DLC ถูกเตรียมโดยเทคนิคแมกนีตรอนสปัตเตอร์ริงแบบแรงกระตุ้นสูง (HiPIMS) เทคนิคโฟโตอิเล็กตรอนสเปคโตรสโคปี (XPS) โดยใช้แสงซินโครตรอนถูกนำมาใช้เพื่อตรวจสอบการปนเปื้อนของฟิล์ม DLC การวัด XAS ในโหมดกระแสอิเล็กตรอนรวมทั้งหมดและการตรวจวิเคราะห์เทคนิต XPS สามารถดำเนินการได้ภายในระบบสุญญากาศเดียวกันในระบบลำเลียงแสง BL3.2Ua ของสถาบันวิจัยแสงซินโครตรอน (SLRI) การปนเปื้อนที่พื้นผิวของฟิล์ม DLC สามารถลดลงได้ด้วยเทคนิคการสปัตเตอร์ริงอาร์กอนไอออนพลังงานต่ำ การวัด XAS ของฟิล์มคาร์บอนคล้ายเพชรนั้นดำเนินการกับตัวอย่างก่อนและหลังทำความสะอาดสำหรับระยะเวลาที่ต่างกัน การปนเปื้อนที่พื้นผิวของฟิล์ม DLC สามารถลดลงปริมาณลงได้ด้วยเทคนิคการสปัตเตอริงอาร์กอนไอออนพลังงานต่ำ การวัด XAS ของฟิล์มคาร์บอนคล้ายเพชรนั้นดำเนินการกับตัวอย่างก่อนและหลังทำความสะอาดสำหรับระยะเวลาที่ต่างกันปริมาณของอะตอมคาร์บอนที่วัดได้มีค่าเพิ่มขึ้น ในขณะที่อะตอมออกซิเจนลดลงเมื่อเวลาสปัตเตอร์ผ่านไป สิ่งนี้ชี้ให้เห็นถึงสารปนเปื้อนพื้นผิวมีปริมาณลดลงโดยการใช้เทคนิคการสปัตเตอร์ริง XAS ของกลุ่มตัวอย่างก่อนและหลังอาร์กอนปัดเตอริง แสดงให้เห็นว่ามีข้อมูลส่วนหนึ่งที่เกิดจากการปนเปื้อน ปริมาณ sp^2 ในฟิล์มคาร์บอนคล้ายเพชรที่ได้จากการวิเคราะห์ XAS นั้นมีความแตกต่างกันไปตามเวลาที่ใช้ในการสปัตเตอร์ริงด้วยไอออน ปริมาณของ sp^2 นั้นน้อยที่สุดในขั้นแรกของการดำเนินงานสปัตเตอร์ริงไอออนจากนั้นจะเพิ่มตามเวลาสปัตเตอร์จนถึงระยะเวลาหนึ่งแล้วลดลงอีกครั้ง การเพิ่มขึ้นของปริมาณ sp^2 อาจเป็นเพราะปริมาณการปนเปื้อนที่ด้านหน้าพื้นผิวลดลง การลดลงของปริมาณ sp^2 หลังจากนั้นอาจเป็นเพราะโครงสร้างบางส่วนเกิดความเสียหายของฟิล์มคาร์บอนคล้ายเพชรที่เกิดจากการทิ้งระเบิดของไอออน ในงานนี้แสดงให้เห็นว่าvขั้นตอนการกำจัด-

ขั้นตอนการกำจัดสิ่งปนเปื้อนบนพื้นผิวที่เหมาะสมจะต้องถูกดำเนินการเพื่อการตรวจสอบความถูกต้องของเนื้อหาคาร์บอนในฟิล์มคาร์บอนคล้ายเพชร

สาขาวิชาฟิสิกส์
ปีการศึกษา 2561

ลายมือชื่อนักศึกษา ____________
ลายมือชื่ออาจารย์ที่ปรึกษา ____________

JIDAPA LOMON : EFFECTS OF SURFACE CONTAMINATION ON XAS
ANALYSIS OF DIAMOND-LIKE CARBON PREPARED BY HIGH POWER
IMPULSE MAGNETRON SPUTTERING SYSTEM. THESIS ADVISOR :
ASSOC. PROF. PRAYOON SONGSIRIRITTHIGUL, Ph.D. 75 PP.

SYNCHROTRON LIGHT/CARBON/DIAMOND-LIKE CARBON /XPS/XAS

This research focuses on the investigations of the effects of surface contamination on x-ray absorption spectroscopy (XAS) that is caused by exposition to air during transfer to analysis chambers. It is inevitable that the surface of the samples was contaminated by absorbed air molecules. In this work the diamond-like carbon (DLC) films prepared by high-power impulse magnetron sputtering technique (HiPIMS). Synchrotron X-ray photoelectron spectroscopy (XPS) was used to verify the contamination of the DLC films. XAS measurements were done in total electron yield mode in the sample XPS analysis chamber of the BL3.2Ua beamline of the Synchrotron Light Research Institute (SLRI). The surface contaminations of the DLC films could be reduced by a low-energy Ar ion sputtering technique. XAS measurements of the DLC films were carried out on the sample before and after ion sputtering for different durations. The quality of C1s photoelectron increases, while the quality of the O1s photoelectron decreases, with the sputtering time. This suggests the reduction of surface contamination by the Ar ion sputtering. XAS of the sample before and after Ar ion sputtering suggests that there is a contribution of information from the contamination. The sp^2 content in the DLC films provided by the XAS analysis varies with the Ar ion sputtering time. The sp^2 content is minimum when on ion sputtering was performed. It increases with the sputtering time up to certain time, the decrease again. The increases of sp^2 may be due to that face that the contamination was reduced. The reduction of sp2 after that may be due to the structural damage of the DLC caused by the ion bombardment. This work demonstrates that proper surface contamination removal procedures must be taken for accurate determination of car bon species in DLC films.

School of Physics Student's Signature

Academic Year 2019 Advisor's Signature Prayoon Song.

ACKNOWLEDGEMENTS

For this thesis, it could not have been accomplished without the support of many people. I would like to express my sincere gratitude for their valuable assistance. Firstly and foremost, I would like to thank my thesis advisor Assoc. Prof. Dr. Prayoon Songsiriritthigul for his continuous support and advice during the course of my M.Sc. study. I feel very lucky and honor to work and study under his guidance.

I express my sincere thanks to Asst. Prof. Dr. Phitsanu Poolcharuansin for providing me the possibilities to learn about HiPIMS and to Dr.Hideki Nakajima for experiences at the BL3.2 beamline. I would also like to thank the BL3.2 staffs at the Siam Photon Laboratory of the Synchrotron Light Research Institute (Public organization) of Thailand: particularly to Dr. Ratchadaporn Supruangnet and Dr.Thanit Sarasota for their help during the photoemission and absorption experiments. I also grateful to thank Miss. Pornthip Chaichompoo for valuable work in the past together.

I would especially like to thank all the faculties and staff members of the School of Physics and colleagues for their assistance throughout the period of this work. This work has been partially supported by the Research Network NANOTEC program of the National Nanotechnology Center, NSTDA, Ministry of Higher Education, Science, Research and Innovation, Thailand.

Finally, I would like to express my deepest gratitude to my parents. For support and encouragement throughout the course of this study at Suranaree University of Technology.

Jidapa Lomon

CONTENTS

Page

CHAPTER

CONTENTS (Continued)

CONTENTS (Continued)

Page

LIST OF FIGURES

Figure **Page**

LIST OF FIGURES (Continued)

Figure **Page**

LIST OF FIGURES (Continued)

LIST OF TABLES

Table **Page**

CHAPTER I

INTRODUCTION

Diamond-like carbon (DLC) is simply one kind of carbon materials that exhibits some of the typical properties of diamond. DLC consists of C atoms with sp^2 and sp^3 hybridizations. The sp^3 hybridized carbon in DLC confers many beneficial properties of diamond, such as high mechanical hardness and chemical and electrochemical inertness, while the sp^2 hybridized carbon controls the electronic and optical properties (Robertson, 1992). DLC has been applied for many industrial applications as protective coatings in various devices, such as in magnetic recording disks, optical windows, cutting tools or micro-electromechanical devices. The outstanding properties of DLC can be controlled by the ratio of sp^2/sp^3 carbons in DLC films. (Ozlem, 2015). In general, different deposition techniques and conditions yield DLC films with different sp^2 and sp^3 ratios. In the past few decades, various techniques have been used to prepare DLC films. One of the most recent techniques that has been received great attention of scientists in the field is high-power impulse magnetron sputtering (HiPIMS). HiPIMS is an extended technique of a magnetron sputtering technique. This technique is considered to be a unique technique. HiPIMS employs high power impulse for the magnetron head. The peak power density of HiPIMS technique is normally higher than 1 kW/cm^2, which is more than a factor of 100 greater than those of conventional direct-current magnetron sputtering systems.

The current density provided by HiPIMS systems is over 1A/cm^2 (Konishi, 2016). Although this technique is in the development phase, the efficiency for preparing DLC films is quite high when compared with other techniques. Along the development of DLC film preparation techniques, there are progresses in characterization techniques and data analyses of DLC films in order to determine accurately the sp^2/sp^3 ratio of the carbons in the films. Different characterization techniques such as X-ray photoemission spectroscopy (XPS), infrared spectroscopy (IR), X-ray absorption spectroscopy (XAS) and thermal desorption spectroscopy (TDS) have been employed. Among those techniques, XAS is one of the most widely used techniques. Normally, an XAS spectrum, absorption coefficient versus photon energy, is used to provide the information of the local structure around the absorbing atoms, carbon atoms for DLC. It is well known that carbon and oxygen are the main surface contaminants for all kinds of solid sample exposed to air. There has been a report on the effect of surface contamination on XAS analysis of graphene and carbon nanorods. Part of the research substantiates that the XAS data affected by surface contamination. XAS analysis indicated that the number of sp^2-C atoms decreased after ion irradiation (Tsukagoshi, 2013) (Shin-ichi, 2014).

This research focuses on the investigation of the effect of surface contamination on XAS analysis for DLC films. It is understood that contamination on the surface on DLC films is unavoidable when the samples are exposed to air during transferring from the deposition chamber to the analysis chamber. There has been no report on the effect of the contaminating carbon on the determination of the sp^2 and sp^3 ratio measured by XAS. Thus, this work emphasizes on this issue.

CHAPTER II

BACKGROUND

This chapter is a summary of the literature review on the topics related to this research. The historical background and preparation as well as applications of DLC films are explained in the first part of this chapter. The research second pant covers the techniques for preparation and characterization of DLC films

2.1 History of diamond-like carbon

During the last few decades, DLC films have been attracted much interest due to their innovative properties such as high hardness, low friction coefficient, high wear resistance, and chemical inertness. These properties can be controlled by the ratio between sp^2 and sp^3 hybridizations of the C atoms. Thus, DLC films were widely used in optoelectronic devices, protective films for tribological or chemical applications, coatings for dies or molds, biological parts and automotive parts and tools (Rajkumar, 2018).

Aisenberg and Chabot discovered DLC by accident during the in experiment on the synthesis in 1971. Their thin films were prepared by an ion beam deposition technique using graphite as the target. Analysis results of the deposited films showed the partial properties and structure similar to diamond such as the index of refraction greater than 2.0, transparency, highly insulating, resistant to corrosion of acid and dielectric constant between approximately 8 and 14, while the diamond is 16.5 and etcetera.

These deposited films were later called DLC (Klaus, 2014). After that, DLC began to draw attention from many researchers because it had many salient qualities**.** Other properties of DLC e.g. low coefficient of friction, high hardness, and chemical stability were reported later. Investigations of new properties and development of preparation techniques for the DLC films are one of the main research topics since the discovery of DLC to date. As present, the unique properties of the DLC films are well-understood. Although a few techniques for DLC films preparation were established, new techniques with batter performance and still demanded.

2.2 Properties and applications of DLC

The DLC film is one of the amorphous carbon clan that synthesized from deposition processes. Most significant feature of DLC is the diamonds bonds in a dense amorphous structure (Robertson, 2002). In general, DLC films are generally classified according to the ratio of the diamond and graphite structure in that sample. The bonding of diamond and graphite structure called sp^3 and sp^2 bonds, respectively. However, the DLC films were often doped with hydrogen, both in the intended and unintentional way. These hydrogen atoms directly affected with some properties of the DLC films. Therefore, the types of DLC depend on the ratio of sp^2/sp^3 hybridizations and H bonds.

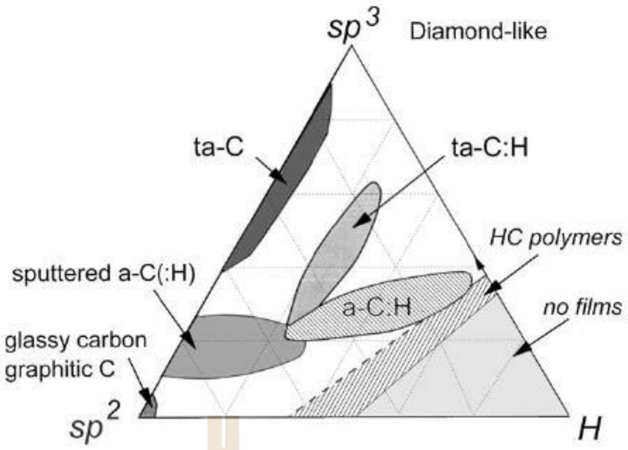

Figure 2.1 Phase diagram of bonding in amorphous carbon–hydrogen alloys (Robertson, 2002).

The DLC types are classified into 7 types as depicted in the phase diagram of DLC materials in figure 2.1, namely:

a) **Polymer-like a-C:H (PLCH):** The film in this group have about 40-60% hydrogen atom volume, which has the highest value among all other types of H atom. The diamonds content can be up to 70 %, but most sp^3 bonds were bonding with the H atom. Therefore, the materials in this group are soft and low density. Their width of the bandgap is 2 to 4 eV. Generally, the film in this group often prepared with deposited by plasma-enhanced chemical vapor deposition (PECVD).

b) **Diamond-like a-C:H (DLCH):** The DLCH film is a group of DLC films that has H content at the middle-level, approximately 20-40%. There is less overall sp^3 content than PLCH films. On the other hand, they have a very high C-C bond that resulting in more mechanical properties. The band gap range from 1 to 2 eV.

c) **Hydrogenated tetrahedral amorphous carbon films (ta-C:H):** The film has general features similar to the DLCH film, but the content of the sp^3 bond greater and the keeping H constant at 20-30%. The density and Young's modulus can be up to 2.4 g/cm3 and 300 GPa, respectively. An optical gap is 2.4 eV.

d) **Graphite-like a-C:H (GLCH):** The film has H content less than 20%, which is the type with the least H atom. Moreover, they have very high sp^2 bonding, resulting in the width of the band gap of less than 1 eV.

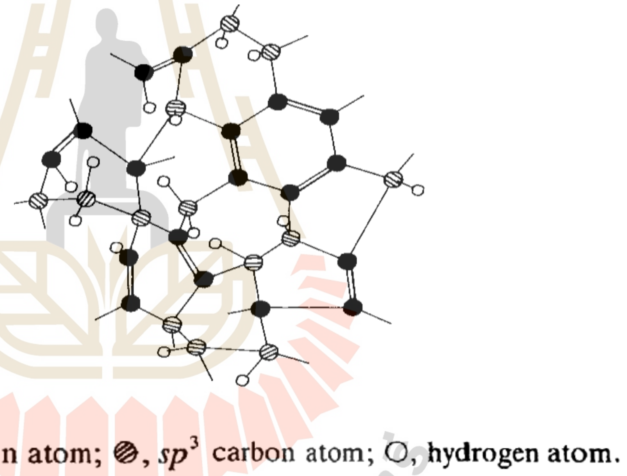

Figure 2.2 A two dimensional representation of diamond like carbon film structure (Robertson, 2002).

Currently, the various structure models of DLC films were proposed, but none is completely accepted. The most common form used to describe the structure of the DLC films is the form that depends on distortion or defects of the graphite structure. This coordination is a function of the hydrogen atom in the film. This model was presented by Angus and Janse, as shown in Figure 2.2. These hybridizations between diamond and graphite in the DLC films are formed disorderly structures that make its properties are changed to a different way.

Table 2.1 Summary of properties and applications of diamond-like carbon films. Text in parentheses indicates potential applications (Grill, 1999).

Property	Type of use	Applications
Transparency in Vis and IR	Optical coatings	Antireflective and wear-resistant coatings for IR optics
Chemical inertness to acids, alkalis and organic solvents	Chemically passivating coating	Corrosion protection of magnetic media, biomedical
High hardness; H=5-80 GPa	Tribological, wear-resistant coatings	Magnetic hard driver, magnetic tapes, razor blades
Low dielectric contents < 4	Low-k dielectrics	(Interconnect dielectrics) (Field emission flat panel displays)
Nanostructure	Very thin coatings <5nm	Magnetic media

It is observed that most structure of DLC films is the structure of diamond or sp^3 bond. This sp^3 bond caused several features similar to the properties of diamond, for example, high hardness and elastic modulus, chemical inertness, corrosion resistance, good thermal conductivity resistance or even biocompatibility and blood compatibility (Grill, 1999). Therefore, DLC is typically utilized the ability of the material for coating applications in various. Whether the optics and electronics fields, the automotive and transportation company, hard discs industry or protective coatings parts. The properties and applications of DLC films summarized followed in table 2.1.

2.3 Deposition Techniques of DLC films

The formation of sp^3 bond in DLC films can occur without hydrogen atom with appropriate conditions. The various techniques were developed to form DLC films preparation methods may be divided into two major categories, i.e. Physical Vapor Deposition (PVD) and Chemical Vapor Deposition (CVD). The PVD method used solid targets for film formation, while the CVD method releases gas to synthesize the film. Both techniques are subdivided into several techniques such as laser vapor deposition, cathodic arc deposition, and sputtering deposition (radio-frequency (RF), direct current (DC) discharge or and self-discharge). This section, the preparation techniques of DLC films employed in this research is explained.

2.3.1 Magnetron Sputtering

Magnetron sputtering is an extremely versatile technique. It is widely used for the preparation of both hydrogenated and hydrogen-free DLC films. In the basic sputtering process, a solid material is used as the target. The target atoms are knocked with high energy ions (plasma ions) that are created in the deposition chamber. These atoms are formed to thin films on the substrate (Helmersson, 2006). Plasma ions are caused by ionization of inert gas such as argon (Ar). These plasma ions are negative, positive or quasi-neutral. For magnetron sputtering technique, the strong magnet is installed behind the target, which may be either a permanent magnet or an electromagnet. When the inertia gas ionized, positive plasma ion is induced by a strong electric field and hits the target. The knocking atom is deposited on the substrate. In a certain case, the electrical connection on the substrate was used to increase the deposition rate. The magnetrons sputtering is divided into direct current magnetron sputtering (DCMS) and radio frequency magnetron sputtering (RFMS).

For DCMS methods, it used of continuous current for creating stable plasma ion bombardment with the target. While the RFMS method often used for insulating materials because of the insulated targets caused charge buildup and reduced efficiency of the process. However, the preparation of the DLC films that using the conventional magnetron sputtering method is relatively low density and content sp^3. This intelligence can be solved by increasing the efficiency of a preparation process but it should not be reduced distinctive point of the original system. Which high power impulse magnetron sputtering technique (HiPIMS) covering all the required features.

2.3.2 High Power Impulse Magnetron Sputtering

The HiPIMS technique is considered as a relatively new technique when compared with the same type of sputtering technique. It was first reported in the year 1999 and was actually used by Bugaev and Fetisov. The basic principles of the technique are similar to the DCMS technique. The most obvious difference is the plasma energy form that used to knock the targets. For the HiPIMS technique, the target is bombarded by high energy plasma for a short time, which is different from the DCMS technique that used continues energy to bombard the target with moderate damage. Moreover, the high energy stimulation of the HiPIMS technique prevented overheats of the magnetic head, which may be breaking the system. The DLC films that prepared by this technique have higher density deposition and homogeneous coating structures. In addition, the capability of the DLC films production may be higher than general techniques. The ability of the HiPIMS technique was confirmed by Meidong and his group. They presented the preparation of graphite-like carbon films by high power impulse magnetron sputtering. Meidong showed the difference of the films prepared by DC magnetron sputtering and high-power impulse magnetron sputtering (HiPIMS), as shown in figure.2.3, The deposition rate and the ratio of sp^2 / sp^3 of GLC films prepare by HiPIMS are higher than those of GLC films prepared by DC magnetron sputtering (Meidong, 2013).

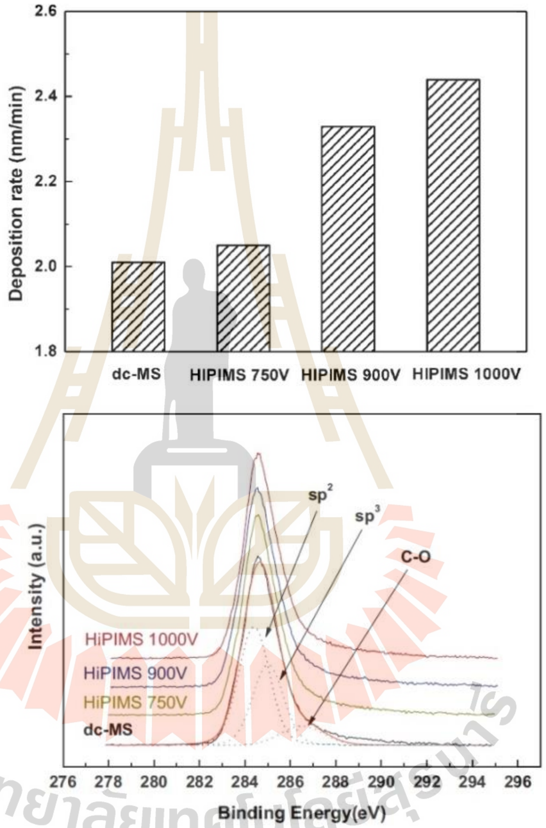

Figure 2.3 Deposition rate of GLC films prepared by DC magnetron sputtering and HiPIMS, b) XPS C 1s peaks of GLC films prepared by DC magnetron sputtering and different with different voltages (Meidong, 2013).

2.4 Characterization Techniques for DLC films

The ratio of sp^2 and sp^3 bonding in DLC are may be approximated by various analytical methods, including X-ray photoemission spectroscopy (XPS), infrared spectroscopy (IR), and thermal desorption spectroscopy (TDS). This section briefly explains common techniques for analyzing the DLC films. However the techniques employed in this work are emphasized.

2.4.1 X-ray photoemission spectroscopy (XPS)

X-ray photoelectron spectroscopy (XPS) seemingly is the most powerful equipment used for analyzing the composition of the DLC films. In the early stages, DLC films analysis of XPS are tricky and needs specialization due to its sophisticated nature. Until 1995, Merel and his group gauged the sp^3 content in DLC films from the decomposition of the C1s. figure 2.4 shows the XPS C1s peaks of DLC samples deposited at different laser intensities.

The sp^3 carbon atom content of DLC films is measured by the ratio of the corresponding peak area over the total C 1s peak area. The spectra in Fig.2.4a distinctly show the DLC C1s compose of at least two components. The higher binding shoulder increases when laser intensity is increased. The Shirley method is used for approximating the contribution of the background, while the fitting of the DLC C 1s peaks is performed by using a mixture of a Gaussian and a Lorentzian.

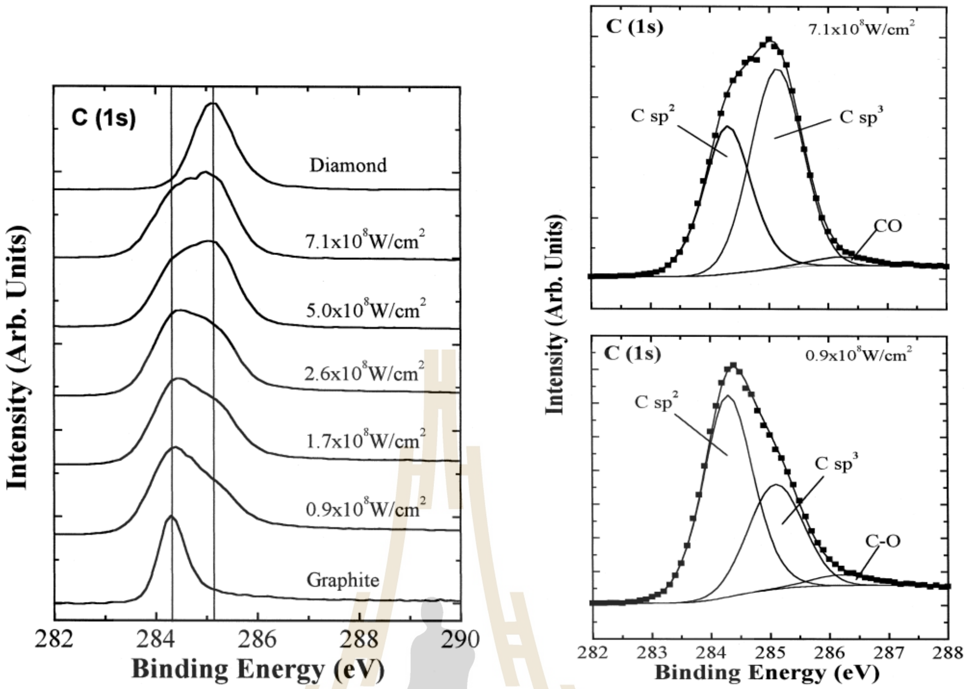

Figure 2.4 a) XPS C 1s peaks of a graphite target,diamond thin film and the DLC thin films obtained at different laser intensities. **b)** Deconvolution of the XPS C 1s peaks of the DLC films deposited at 0.9×10^8 and 7.1×10^8 Wrcm^2 (Merel, 1995).

The fittings for the samples deposited at the highest and lowest laser intensity are presented in figure 2.4a. The C1s XPS spectra are separated into least two different main components, at 284.4 eV and 285.2 eV, which corresponds to sp^2 and sp^3 hybridized carbon atoms, respectively. From the deconvoluted spectra, the ratio of the corresponding peak area over the total C1s peak area is used to determine the sp^3 carbon atom content. At present, this method is reliable and widely recognized (Merel, 1995). Normally, XPS is a one of highly surface-sensitive technique, thus cleanliness of surface are essential. For a detailed characterization with highly surface-sensitive methods, surface analytic studies are mostly performed under ultrahigh vacuum (UHV) conditions. Although the pressure of the residual gas is very low under UHV conditions, the surfaces are never kept permanently clean (Steinberger et al., 2017). Therefore, XPS analyses have been used in combination with sputter ion etching for cleaning contamination on surfaces.

It is well known that XPS is one of the most reliable techniques to analyze the structure of the DLC films. This technique is a surface-sensitive technique, which must be careful of surface contaminants on the sample. On the other hand, the surface contaminants can also use to identify by this technique. The above information is confirmed by Zemek and group (Zemek, 2016). The effects of argon sputtering on XPS analysis of DLC and nanocrystalline diamond film surfaces are studies. The sp^2 and sp^3 hybridization of DLC films before and after cleaning surfaces are presented. Zemek and his research team used high-energy resolution core-level XPS for examining the influence of argon cluster ion beam on composition and chemical bonding of DLC and nanocrystalline, focusing on the peak widths and hybridization of carbon atoms which are evaluated from C1s lines.

Changes in the FWHM values of nanocrystalline diamond (NCD) samples reflect structural disorder induced by Ar cluster ion bombardment than the changes in the C sp^2 and C-O contributions, as shown in figure 2.5. The contaminants on the surface are detected at the first spectra or C1s XPS spectra before bombard surface by Ar cluster ion. Changes of FWHM values and shape of XPS spectra before and after Ar cluster ion confirmed that the contaminants are removed (Zemek, 2016).

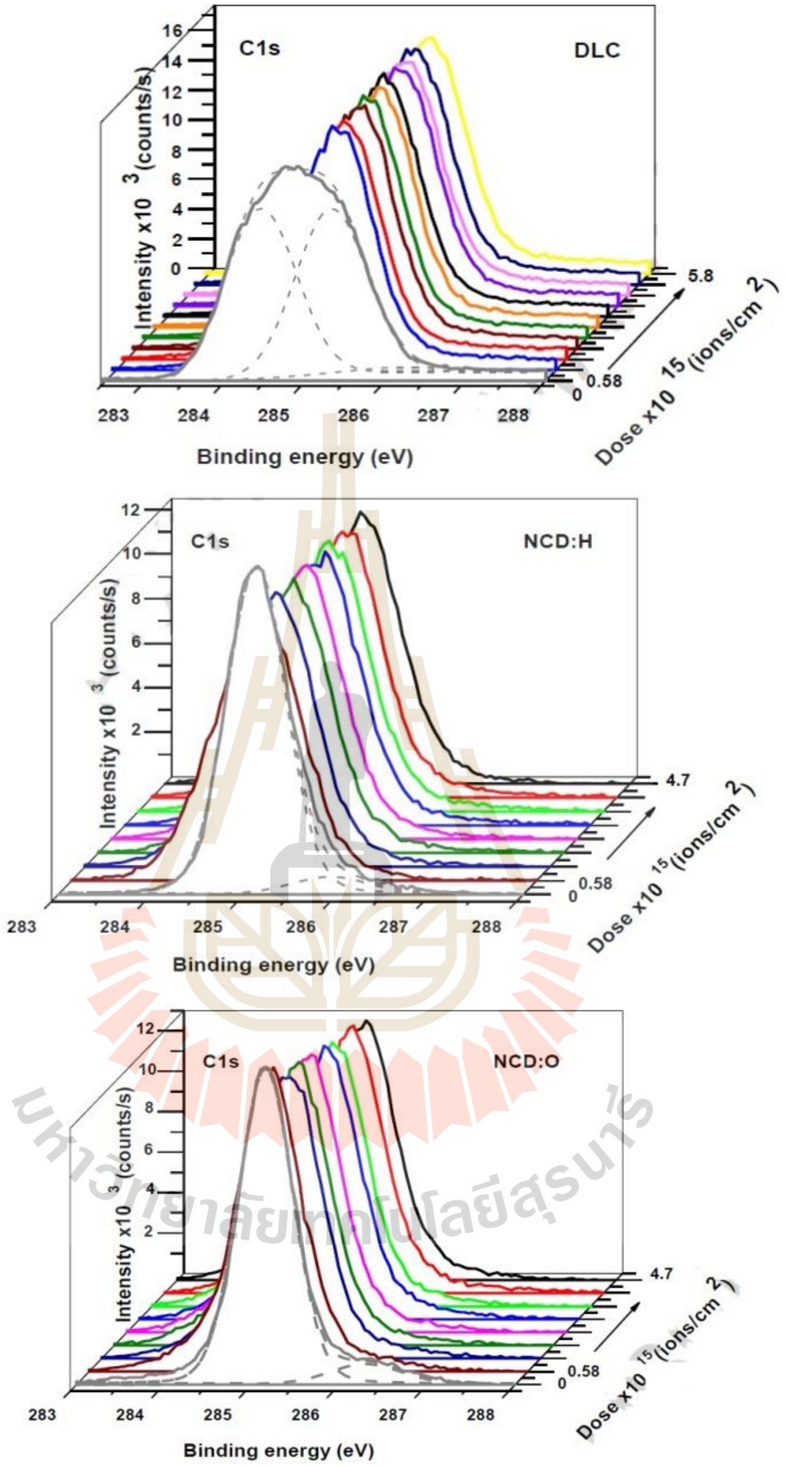

Figure 2.5 High-energy resolution C 1s spectra recorded from as-received and Ar cluster ion sputtered DLC (a), NCD:H (b), and NCD:O (c) Samples Zemek, 2016).

2.4.2. X-ray absorption spectroscopy (XAS)

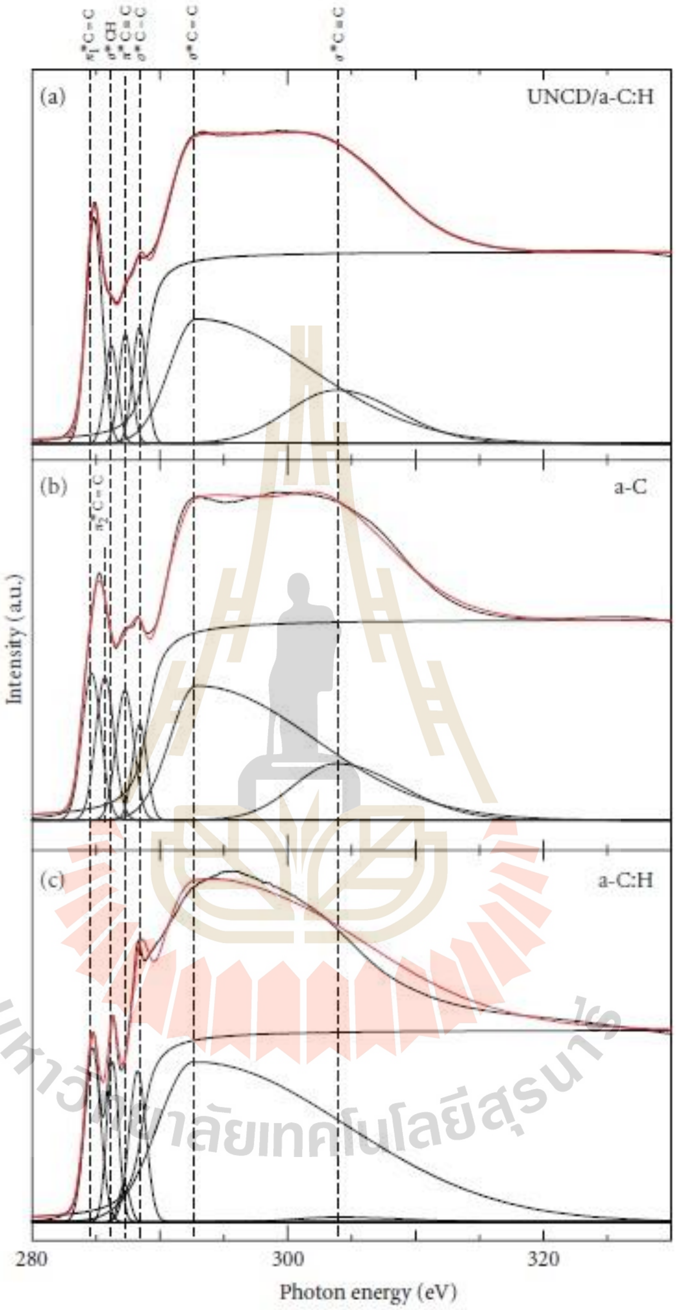

Figure 2.6 Experimental and fitted NEXAFS spectra of (a) UNCD/a-C:H film deposited, (b) a-C film deposited, and (c) a-C:H film (Shinya, 2009).

XAS technique has recently been well accepted for characterization of various carbon films due to the ability to provide information with high accuracy on the local structure surrounding excited carbon atoms and the orientation of the carbon bonds. In the beginning XAS, investigations of the local bonding configurations within an amorphous carbon of XAS technique were judged by the features of x-ray absorption spectra (Lenhart, 2005). Until 2009, Shinya and his group successfully utilized for investigating the local bonding configurations within amorphous and nanocrystalline carbon by deconvaluting near-edge X-ray absorption fine structure (NEXAFS) (Shinya, 2009). The absorption spectra of carbon films were deconvoluted to identify different bonding configurations such as π∗ and σ∗ bonds. The NEXAFS spectra of the UNCD/a-C:H film, a-C film, and a-C: H film deposited are shown in figures 2.6 (a), (b), and (c), respectively. The red solid line is a spectrum from fitting. In data analysis, the experimental data is subtracted by an error-function step, which is originated from the C K-edge at the ionization potential. The subtracted spectrum decomposed into Gaussian peaks corresponding to π∗C=C, σ∗C–H, π∗C≡C∗, σ∗C–C, σ∗C=C, and σ∗C≡C. (Shinya, 2009).

At present, investigating the local bonding configurations by XAS technique has been accepted and extensively used. In general, C K-edge spectra consist of the transition peaks and ionization function. The ratios of the sp^2 and sp^3 bond are estimated by the ratio of the corresponding peak area over the total C K-edge peak area. C K-edge spectra of tetrahedral amorphous carbon (ta-C) thin film (one of DLC structure), as shown in figure 2.7, comprise seven peaks corresponding to, π∗ sp^2, ketone/aldehyde, C-H, carboxyl, sp^3, Rydberg states and σ∗ sp^2 at 284.9 , 286.6, 287.5, 288.6, 289.8, 291.0 and 292.8 eV respectively (Sainio et al., 2016).

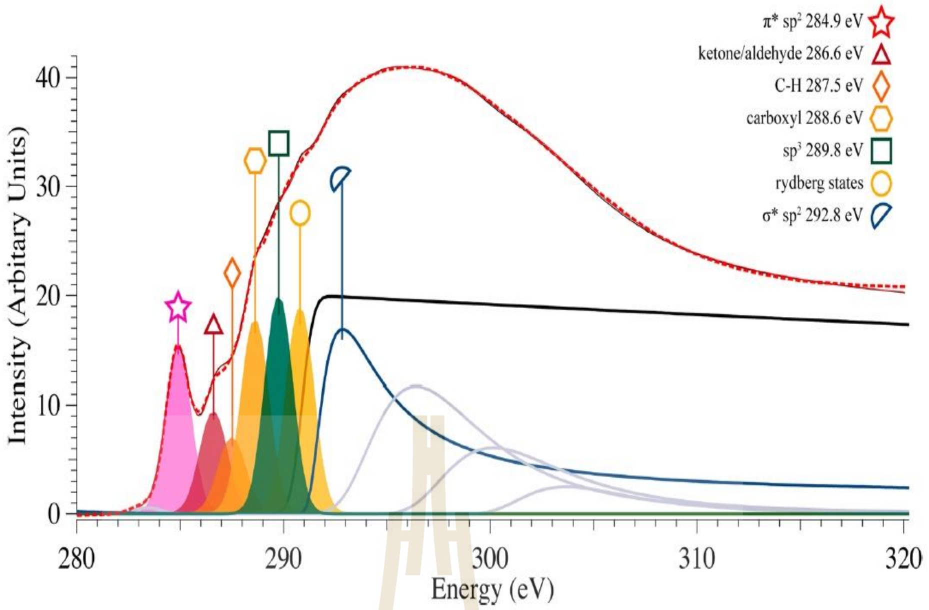

Figure 2.7 Measured (black dotted line) and fitted (red line) C k-edge token from ta-C film (Sainio, 2016).

There have been many reports on the comparative studies between XAS and XPS techniques (Quiros, 2015). N k-edge XAS and N 1s XPS of carbon nitride film showed in Figure 2.8. Quiros and his group reported the analysis of amorphous carbon nitride films by XAS and XPS techniques. Changes XPS and XAS spectra by annealing treatments is observed. Carbon nitride films are grown with different sputtering and assistance conditions. Their surface N/C atomic ratios are 0.3 and 0.5. Figure 5 shows the N 1s XPS and N k-edge XAS spectra of the sample with nitrogen content before and after annealing. The comparison of figures 10 suggests a correlation between the low binding energy components of XPS, at 399.3 eV, with transitions 399.6 and 400.8 eV of XAS spectra. (Quiros, 2015).

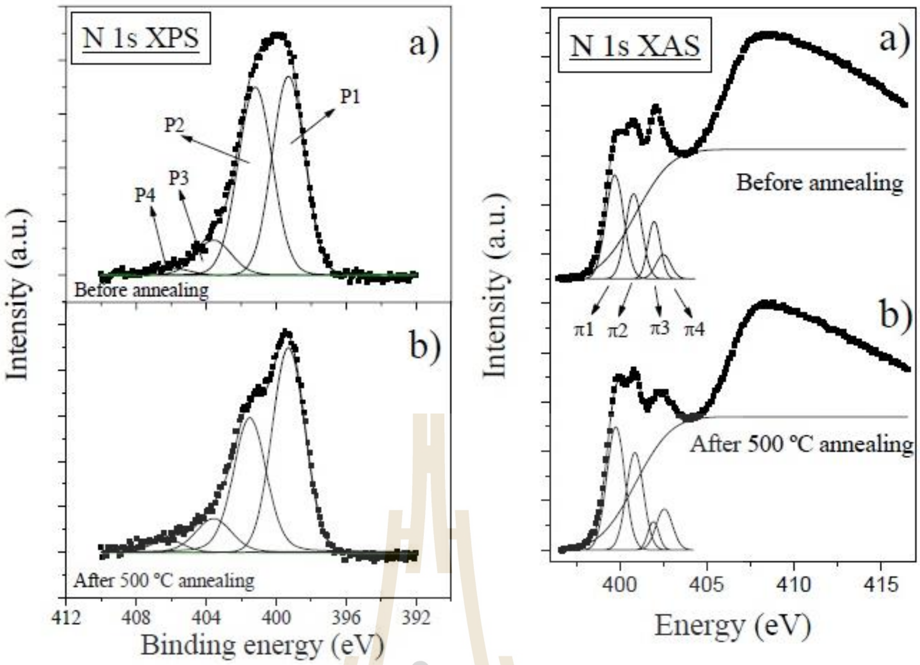

Figure 9 The XPS N 1s and XAS N k-edge spectra of the sample with nitrogen content before and after annealing (Quiros, 2015).

From the literature review above, it can be seen that both XAS and XPS techniques are accepted and used in various researches. However, there has been reported about the XAS technique that may be a problem for its reliability. For measurements with XAS techniques, the experiments were performed under ultra-high vacuum pressure. Most experiments measured without ignoring the surface contamination. However, the effects of surface contamination on a carbon sample that measure by XAS techniques were reported. Tsukagoshi and his group reported about the damage of multiwall carbon nanotubes to amorphous carbon nanorods under ion irradiation. One of his interesting results is the change of graphenes spectra before and after ion irradiation at low ion irradiation energy. This energy range is the energy level for normally used cleaning the surface of the sample. It can be seen clearly that there is a change in the intensity of the π^* peak shown in figure 2.8. In general, the

XAS technique for DLC characterization is in a total-electron yield mode. Inevitably, the XAS spectra contain signal from surface contamination. This is an interesting distinction.

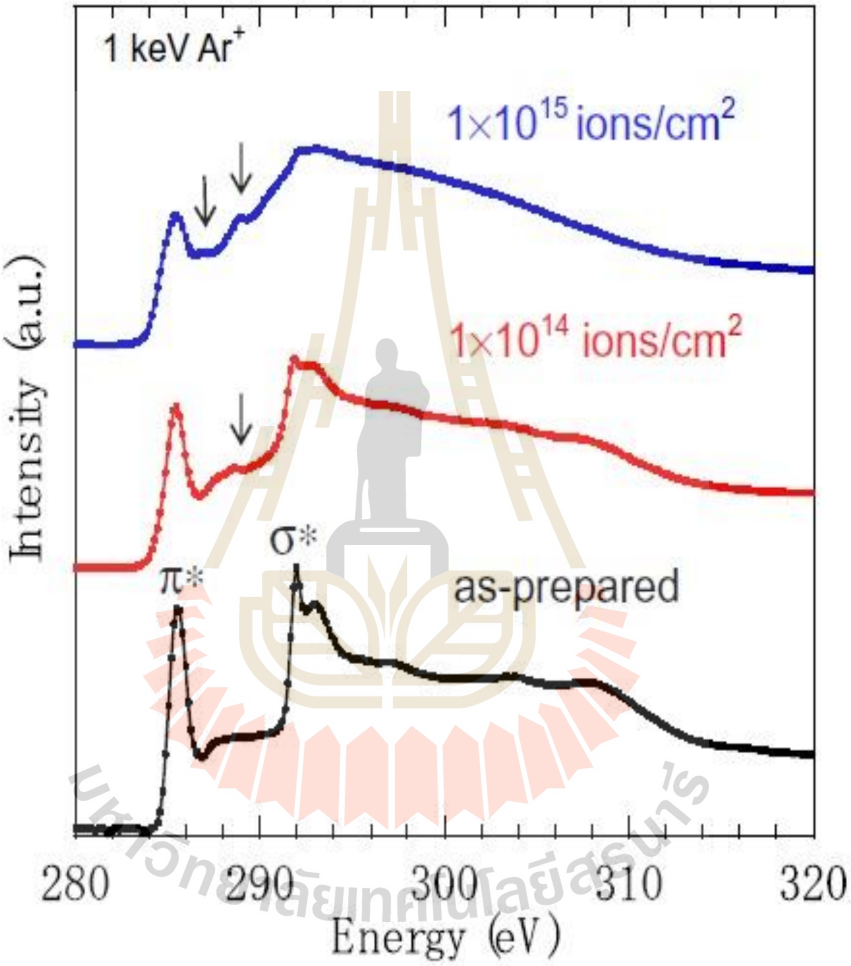

Figure 2.8 The XAS spectra of graphenes irradiated at an energy of 1 keV (Tsukagoshi, 2013).

It can be seen that this effect can be clearly observed in carbon materials. The DLC films are a type of carbon material which this effect may also appear in DLC sample. However, the causes of change in the XAS spectrum cannot be clearly identified due to changes that can be observed in Tsukagoshi report may be caused by some destruction of the sample. To explain this spectrum change is an interesting question. Preliminary prediction of this change is the impact of surface contamination on the sample. Generally, most carbon samples are sensitive to the atmosphere. Air molecules are often detected as an unwanted surface contamination. These contaminations is usually formed when the sample are exposed to air.

CHAPTER III

EXPERIMENTAL

In this work, the DLC films were prepared by a high power impulse magnetron sputtering technique surface contamination on the DLC films were identified by X-ray photoelectron spectroscopy (XPS). The effect of surface contaminations on the DLC films on XAS analysis was studied by comparison of data from the DLC samples before and effect surface cleaning. It is noted that measurements were certified at the XAS experiment will be measured in the same XPS system. The details of the experimental procedures are as the follows.

3.1 Materials

Materials used in this experiment consist of 99.99% graphite Sputtering Target (3 inches), gas argon, gas nitrogen, glass slides, DI water and ethanol 99.99%.

3.2 Deposition Procedure

3.2.1 Deposition system

The DLC films have been synthesized by the HiPIMS technique. A schematic of the deposition chamber is shown in figure 3.1. The plasma glow system comprises a cylindrical stainless steel deposition chamber with dimension of 45 cm in diamante and 56 cm in length. The substrate holder is a stainless steel sheet of 12 cm diameter connected to a stainless steel rod for adjusting the distance, approximate diameter 2 cm. The base pressure in the deposition chamber was maintained at 2.7 × 10^{-5} mbar, by using two types of pumps; scroll pump for evacuations the pressure from the atmospheric pressure to 10^{-2} mbar and turbo pump for making pressure into base pressure. Operating pressures in the deposition chamber were controlled by the flow rate of the Ar gas. The plasma was produced by HiPIMS power supply and a shutter was used to stop the unwanted deposition. The densifications or intensifications of plasma were controlled by changing the parameters in the deposition of the DLC films.

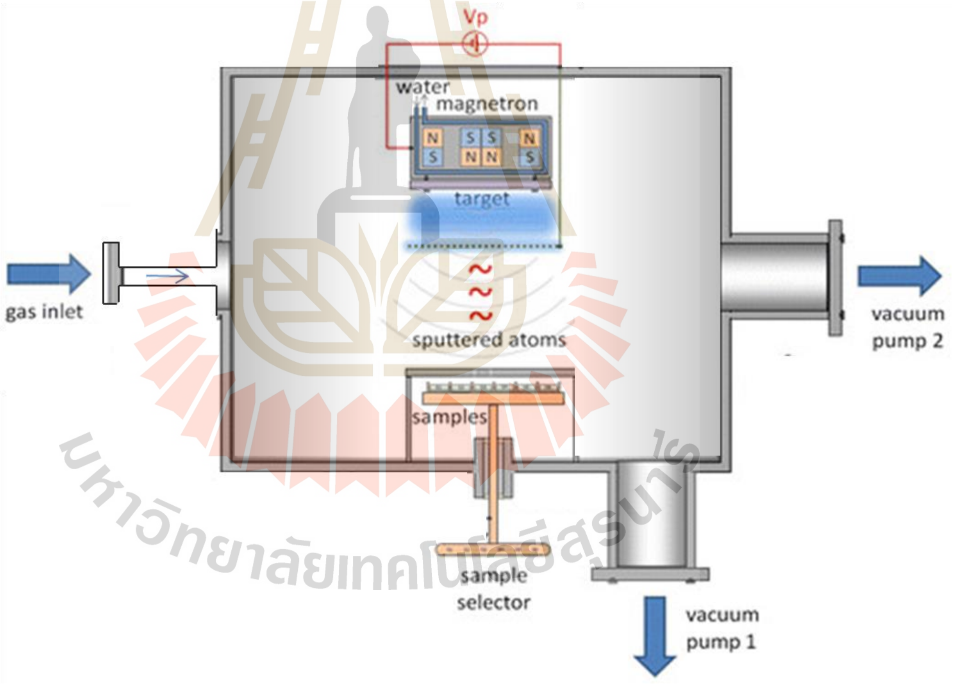

Figure 3.1 A schematic of the deposition chamber.

3.2.2 Procedure for deposition of DLC Films

Microscope slide glasses were used as substrates with dimensions of 2×2 cm^2. The substrates were gently cleaned successively with ethanol and then with DI water in an ultrasonic bath for 30 min each. The substrates were dried by N_2 gas before being loaded into the deposition chamber. DLC films were deposited by HiPIMS technique. The deposition time was 60 minutes and the average power was 157 watts. The target is pure graphite with 3 inches in diameter. The distance between the targets to the substrate was 11 cm. The flow rate of Ar gas was 10 sccm. The base pressure and operating pressures were 2.7×10^{-5} and 2.2×10^{-2} mbar, respectively.

3.3 Characterization techniques

3.3.1 Synchrotron radiation

3.3.1.1 Synchrotron

A synchrotron is a large machine that accelerates charged particles e.g., electrons and ions to the speeds close to that of light. As these electrons or ions are deflected by magnetic fields they create highly electromagnetic radiation, called synchrotron radiation or synchrotron light. The principal structures of the synchrotron presented in figure 3.2. In the first stage, the electrons generating from the electron gun (1) are accelerated in the linear accelerator (linac) (2). The radio frequency is used to acceleration electrons, this wave creates intense electric and magnetic fields. When the electrons enter the linac, the intense electric field are switched back and forth between negative potential and positive potential (Wilson, 1996).

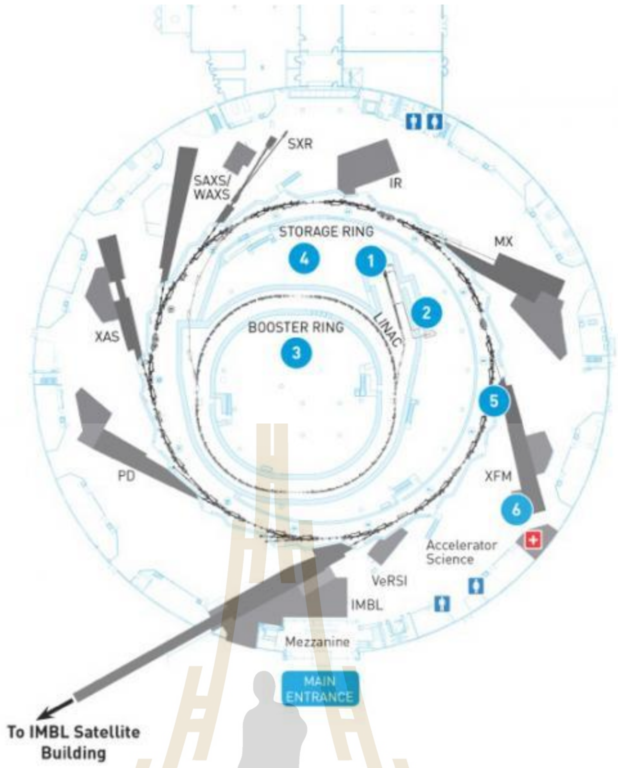

Figure 3.2 The principal structures of the synchrotron (ANSTO group, 1997).

Charged particles (electrons) are pulled by this change of electric field and are accelerated to the speed of light. In the second stage, they are transferred to the booster ring (3) and are accelerated the energy range up to giga-electron volts while adjusting the magnetic field corresponds to the energy of the electrons to maintain the radius of curvature of the electric. Then they are transferred to a circular storage ring (4). When electrons are deviated in the storage ring by the magnetic field, the synchrotron light is emitted tangentially to the electron orbit. This radiation is transported into the beamlines (5) for use with various experiments. In general, synchrotron radiation covers a wide range of wavelength (over 4 types, consists of infrared, visible light, ultraviolet, and x-rays). This radiation is high intensity or over millions of times brilliant than other light sources.

3.3.1.2 The uniqueness properties of a synchrotron radiation.

The proportion of synchrotron radiation properties are rather unique, as summarized below.

Wide continuous spectrum and adjustability: the spectrum of synchrotron radiation produced by a bending magnet is continuous. The spectrum range of the synchrotron radiation is shown in figure 3.3. This spectrum covers from infrared up to hard X-rays. Since the spectrum of synchrotron includes all wavelengths, it often called to as white light. Moreover, synchrotron radiation can be selected with appropriate energy range for each material, therefore it becomes an adjustable radiation source.

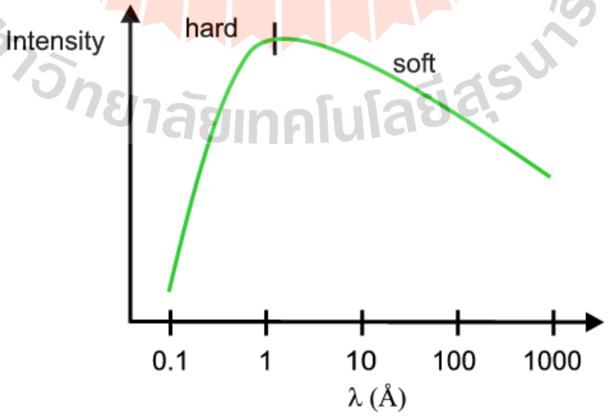

Figure 3.3 The spectrum range of the synchrotron radiation (Paul, 2006).

Polarization: The synchrotron radiation emitted from a bending magnet is horizontally polarized at linearly polarizing in the plane of the storage ring, while the emission synchrotron radiation above and below the orbit is circularly polarized. As shown in the figure 3.4, the vibration of synchrotron sources is horizontally polarized but the X-ray radiation from laboratory sources is vibrating in all planes. This feature has advantages for investigations of magnetic materials.

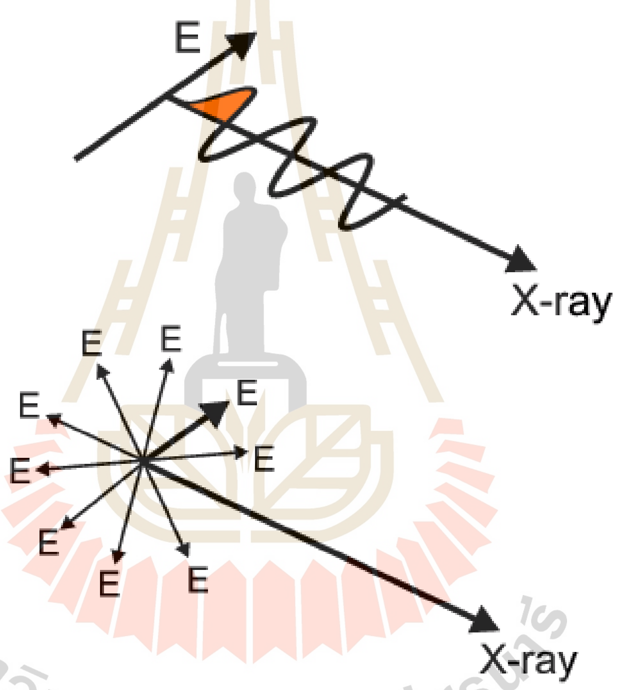

Figure 3.4 the synchrotron radiation in horizontally polarized and circularly polarized (Paul, 2006).

Very high intensity (flux) and high brilliance: Photon flux of synchrotron radiation is very high. In general, the flux depends on the number of electrons circulating in the ring per unit time (beam current), which synchrotron radiation has very high beam current more than of conventional X-ray source. The high flux and high brilliance of synchrotron radiation can be used for measuring the infinitesimal and diluted samples as well as data high-resolution.

Pulsed character: Synchrotron radiation is not actually continuous but it is emitted in short bursts time. The pulsed property of the synchrotron radiation can be used for study in some specialized experiments (Paul, 2006).

3.3.1.2 Synchrotron light research institute (SLRI)

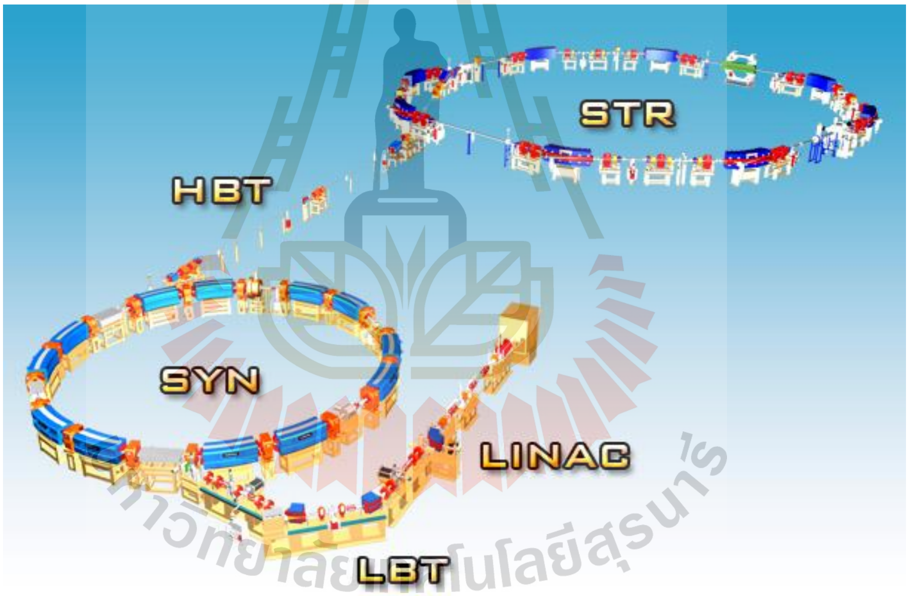

Figure 3.5 the main component of the Synchrotron Light Research Institute.

Synchrotron Light Research Institute (SLRI) is the first synchrotron radiation research facility in Thailand. The current location is the Technopolis of Suranaree

University of Technology, Nakhon-Ratchasima. The main components of the light source at SLRI are shown in Figure 3.5. The electrons accelerated in the linear accelerator (LINAC) up to a 40 MeV. These electrons are transported by the low energy beam transport line (LBT) before entering to booster synchrotron (SYN). Radio Frequency wave (118 MHz) is used for the acceleration of electrons to produce electrons with energy of 1.2 GeV. Then, these electrons are consigned to the storage ring (STR) by the high energy beam transport line (HBT). Currently, there are 10 beamlines providing various measurement techniques such as X-ray Absorption Spectroscopy (XAS), Infra-Red Spectroscopy (IR), Photoemission Spectroscopy (PES), X-ray Fluorescence (XRF) and Deep X-ray Lithography (DXL).

3.3.2 X-ray photoelectron spectroscopy (XPS)

3.2.2.1 Principle of XPS

X-Ray photoelectron spectroscopy (XPS) is one of surface analysis techniques with a probed depth approximately 2 to 5 nanometers (nm) from the surface. XPS can reveal chemical species of the atom at the surface region. It relies on photoelectric effect. Soft x-rays irradiated on a sample excite electrons in core level to vacuum states. The kinetic energies of these excite electrons depends on the binding energy and the exciting photon energy. A general XPS spectrum presents the number of emitting electrons in each kinetic energy or binding energy. Since the binding energies are specific to the element. The photoelectron can be used to identify the elements in the materials.

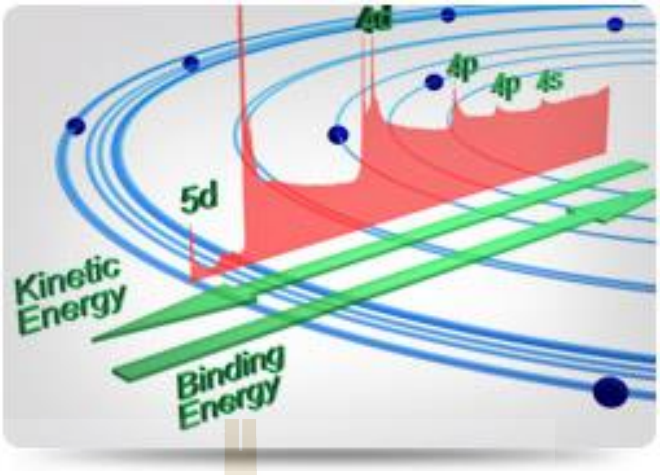

Figure 3.6 the electronic state exists in the atom.

As shown in figure 3.6, the electronic states existing in the atom (e.g., 1s, 2s, 2p, 3s, etc.) are presented in each XPS peak. The XPS peaks show Gaussian-Lorentzian curves. The breadth of FWHM is a determinant of chemical bond in samples due to having various factors affect to magnitude of FWHM e.g., the resolution of the detector or size of an X-ray beam, etc. The kinetic energy of emitted photoelectrons is given by the fowllowing equation

$$E = E_k + E_B + \emptyset, \tag{3.1}$$

where E is the photon energy, E_k is the kinetic energy of the electron after being ejected, E_B is the binding energy of the electron in the material and $\emptyset$ is the work function of the material. The work function is defined as the minimum energy required for an electron to escape from the material. Typical work functions are on the order of a few eV whereas core electron binding energies can range from ~10 eV up to a few keV. Therefore excitation of a range of orbitals in most elements is commonly done by using soft X-rays (~200-2000 eV). The process is illustrated in figure 3.7. For a conducting sample in electrical contact with the analyzer, the Fermi levels of both are equal. In this case, the work function in equation 3.1 corresponds to that of the analyzer. For insulators or samples which cannot be grounded, this is not the case. In order to achieve accurate binding energies, reference peaks of well-known energy can be used to calibrate the spectrometer.

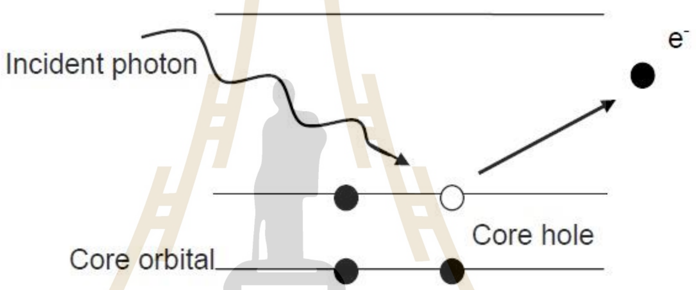

Figure 3.7 A schematic diagram of the photoelectric process. An incident photon causes an electron to be ejected from an atomic orbital according to eq. (3.1).

XPS is the surface sensitivity technique since the inelastic mean free path of the photo electrons, λ is rather-short. This can be explained by Beer-Lambert law.

$$I(x) = I_0 \exp\left(\frac{-x}{\lambda cos\theta}\right), \tag{3.2}$$

where I(x) is the intensity after traveling through distance x, I0 is the initial intensity and θ is the angle from the emitting angle of the photoelectron with reference to surface normal. λ is a Inelastic mean free path. Approximately 99.7% of photoelectrons that excited from core electrons came from 3λ of depth or the depth of a few nm from the surface. The experimental mean free paths of elements in different material are compiled in figure 3.8 (Biesinger, 2018) (Mohai, 2000).

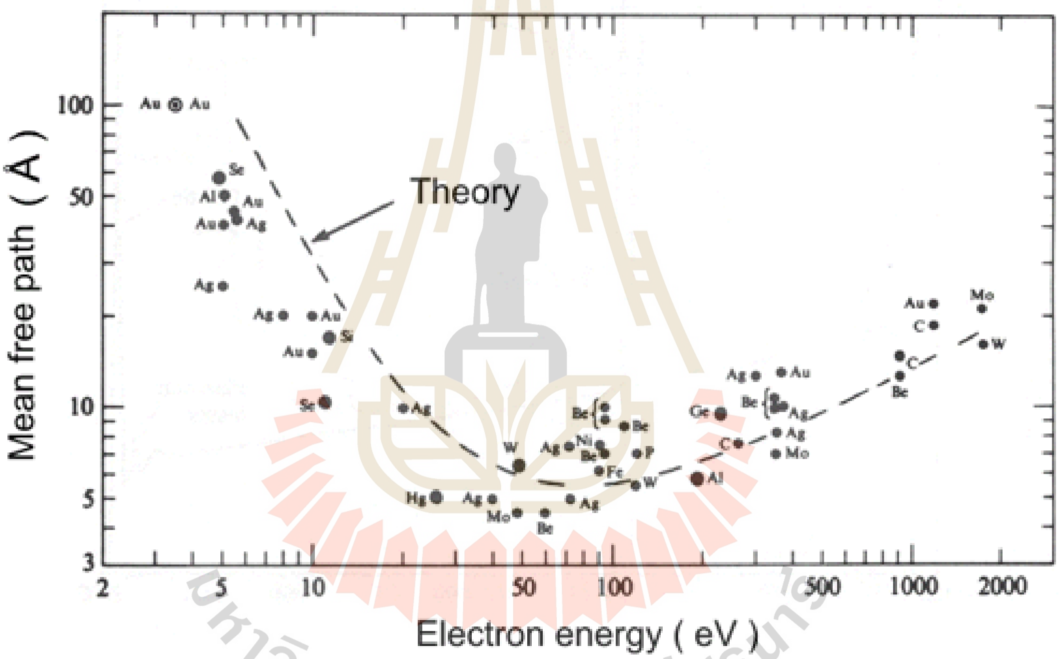

Figure 3.8 The universal inelastic mean free path curve (Raúl, 2000).

3.3.2.3 Chemical shift

XPS survey spectra are normally used to identify the presence of elements in the samples. Detailed scans of specific orbitals may reveal a number of convoluted peaks with different binding energies, a product of different chemical shifts as seen in figure 3.8. Chemical shift arises from the presence of atoms bonded in different chemical environments such as bonding to different elements or differing oxidation states. The spectra can be deconvoluted using data processing software to fit a number of Gaussian-Lorentzian peaks to reconstruct the data, different chemical environments can be identified according to the respective binding energies of these peaks.

3.3.2.4 Sample charging

When working with insulating samples it is often not possible to have the sample in electrical contact with the analyzer. Electrons which leave the surface are not replaced, leading to sample charging. Charging can lead to significant shifts in expected peak positions as photoelectron energies are altered by the resulting electric field and can cause broadening or splitting of peaks if the charge of the sample surface is heterogeneous, known as differential charging. For spectrometers with a non-monochromated X-ray source, the effects of charging are reduced somewhat by a steady flow of electrons from the anode but these electrons are not present when using a monochromator.

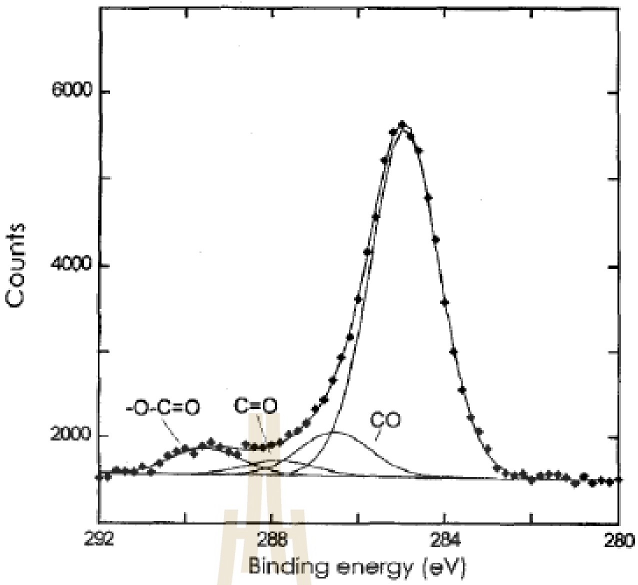

Figure 3.9 A narrow scan over a C 1s region showing chemically shifted components as a result of different bonding configurations with oxygen (Blackmore, 2004).

3.3.3 X-ray absorption spectroscopy (XAS)

3.3.3.1 Principle of XAS

X-ray absorption spectroscopy (XAS) is admittedly technique used extensively for determining the local geometric or electronic structure of material. Generally, after the electron has been ejected by X-ray, a core electron is excited to a vacant energy level or ejected from the atom. Electrons from another-shell then fall into a core hole, the photons that are emitted have a unique absorbance of energy levels with each element. Generally, XAS typically used absorbance in the material to deduce information about the atomic local structure. After the electron has been ejected by X-ray, a core electron is excited to a vacant energy level or ejected from the atom. Electrons from another-shell then fall into a core hole, the photoelectrons that are emitted have a unique absorbance of energy levels with each element, as show in figure 3.10. These photoelectrons are also presented information about the local structure of the neighbor atom that can be applied to deduce the local structure of atoms. However, XAS required high-energy X-ray excitation for exciting the electrons from the core-shell. Therefore, the XAS is one technique that uses the synchrotron light source. The typically X-ray energy is about 104 eV, range between 100 eV- 3 keV are soft x-rays that used for low Z elements matter such as carbon (285 eV), nitrogen (400 eV) and oxygen (530 eV) and hard x-rays are above 3 keV.

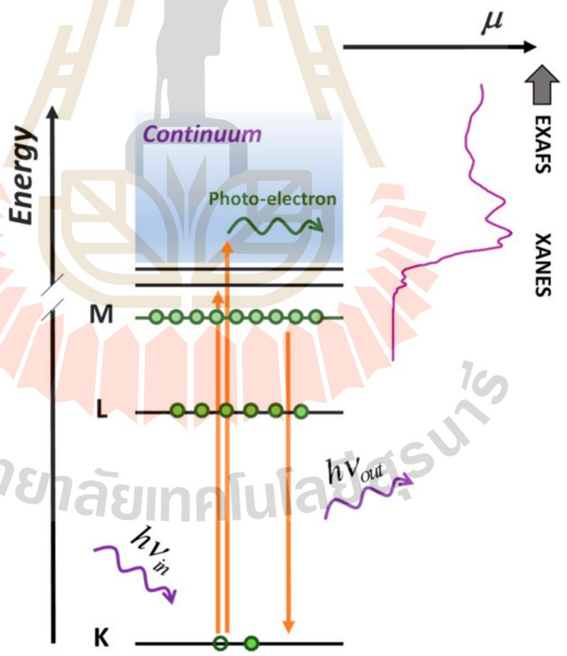

Figure 3.10 Scheme of the X-ray absorption process (Stöhr, 1992).

As present in figure 3.11, the emitted electrons are from adsorbate and substrate. Generally, soft X-rays source can penetrate into the sample around 1 μm.

The photoelectrons and Auger electrons are creating before reaching to the surface by the absorbed X-rays. The electron-electron interaction of these electrons is scattered inelastically. The inelastic scattering of the electrons results in some electrons cascade. When the electron reaches the surface, the electrons with energy higher than the work function will escape into the vacuum. The electrons emerging from the surface are detected.

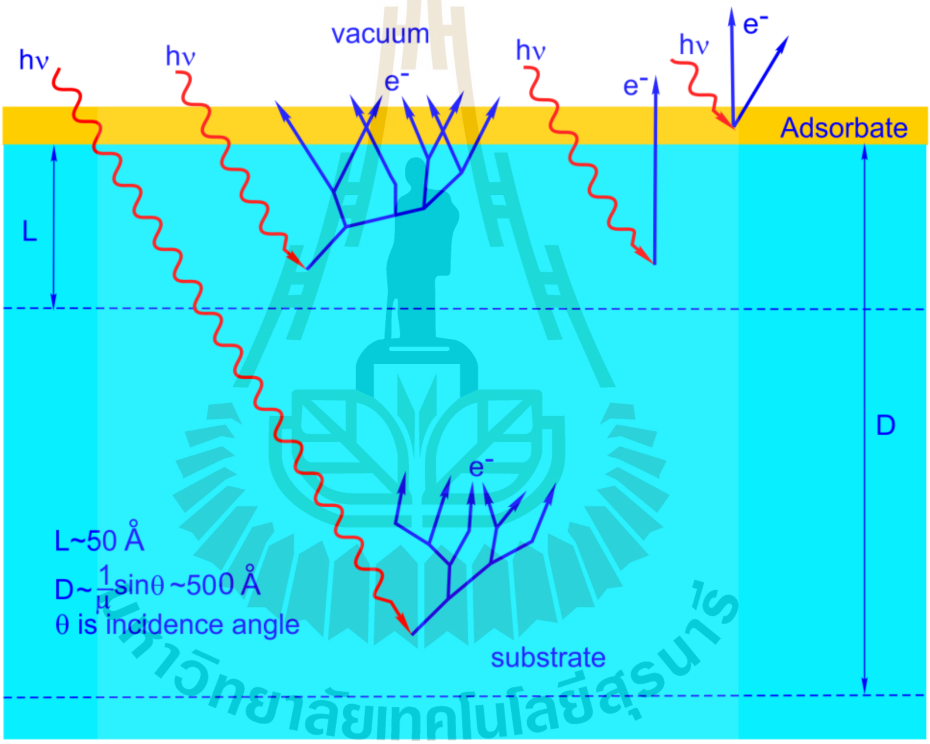

Figure 2.13 Photon penetration depth D (depends on absorption coefficient μ and radiation incidence angle θ) and inelastic mean free pass L of electrons. Adopted from (Stöhr, 1992).

3.3.3.2 Molecular orbital

Molecular orbital theory (MO) is a wave function describing the electron distribution around nuclei. The formation of molecular orbitals by a combination of their atomic orbitals caused facilitation of the bonding between atoms. The electrons are not assigned to one particular atomic bond but considered to be distributed across the whole molecule. For each MO, a maximum of valence electrons is two electrons with opposite spins. The MO with the lowest energy is filled first. Molecular orbitals are subdivided into different types according to their symmetry. σ orbitals are molecular orbitals that are symmetrical about the axis of the bond. The diagram of the simplest MO diagram for the hydrogen atom is presented in Fig. 3.12. The 1s orbitals of two hydrogen atoms caused one bonding σ orbital and one anti-bonding σ* orbital.

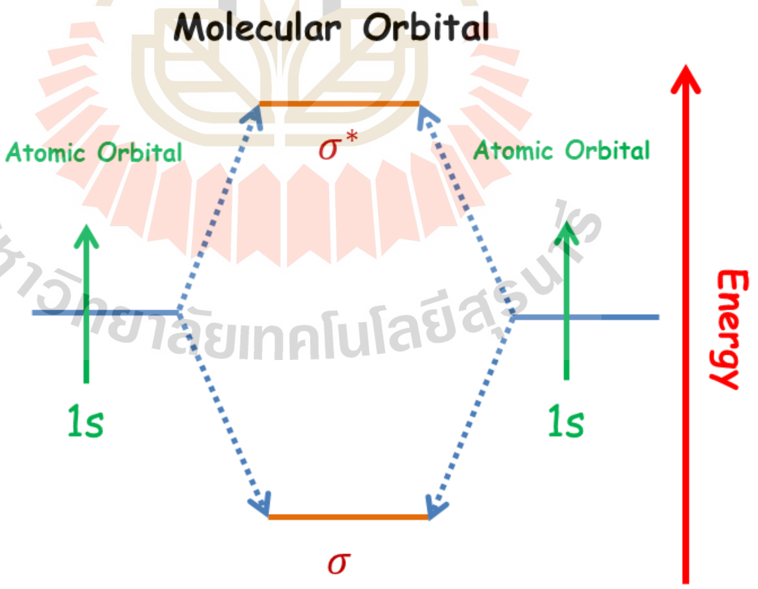

Figure 3.12 The MO diagram of the hydrogen molecule. Two 1s atomic orbitals form two σ molecular orbitals.

3.3.3.2 XAS sensitivity to molecular orbitals

Figure.3.13 illustrates a typical K-edge spectrum for a molecular of two atoms. The XAS spectrum shows the resonances 1s* comprising of the lower energy region and a high-resolution region. The resonances corresponding to 1sπ* transitions have a broader pattern at higher energies above the absorption edge. Usually, the information about molecular orbitals does not appear at the π* resonances and the absorption edge. Moreover, the 1s π* resonance specifically correspons to the molecules with a double and triple bonding. Thus, the 1s π* resonance does not appear in single bond molecules. (Stöhr, 1992)

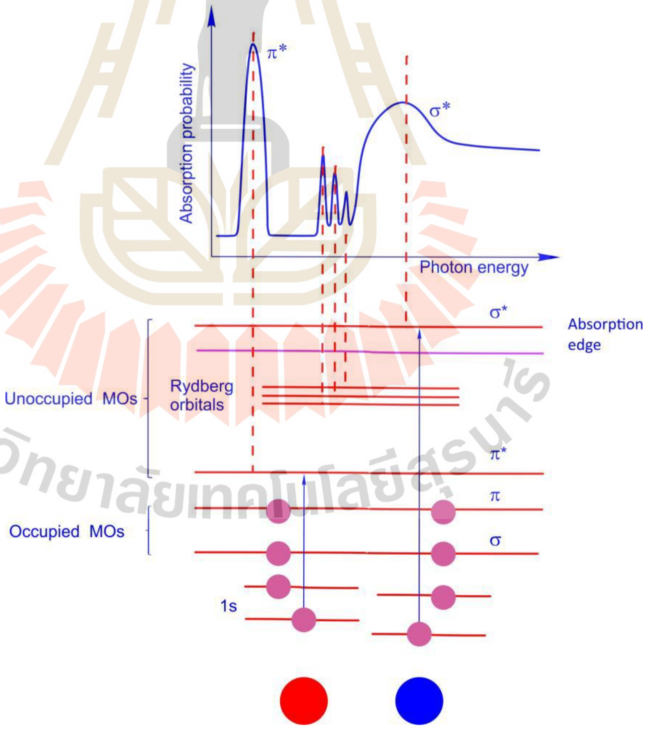

Figure 3.13 Diatomic subunit with the corresponding 1s-π* and 1s-σ* transitions and typical NEXAFS spectrum profile. Modified from (Georg, 2006).

3.3.3.3 Normalization and Background Subtraction

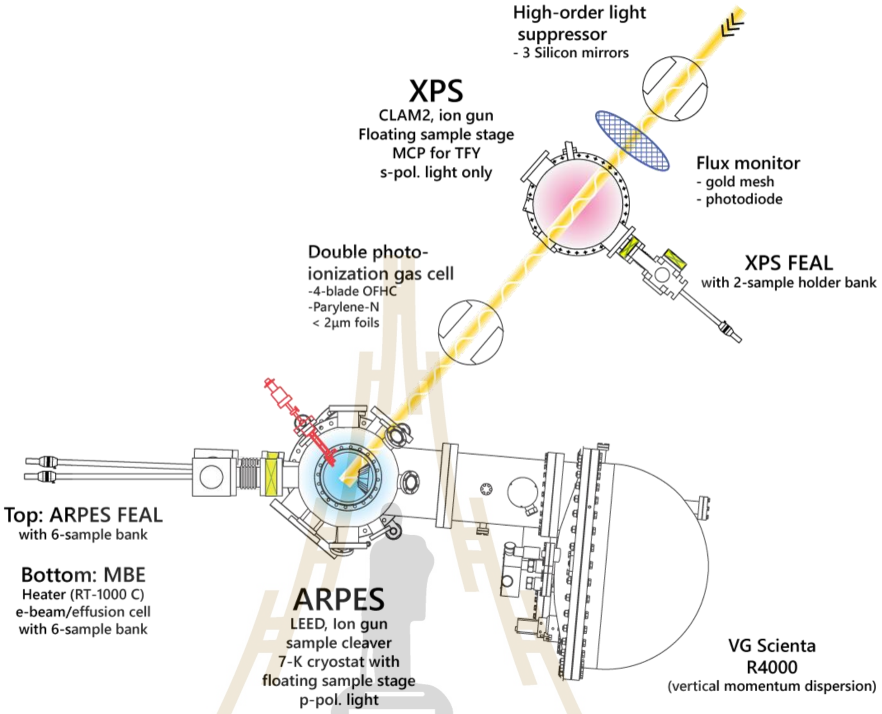

Figure 3.14 Generalized schematic diagram of the XAS experiment Bl3.2a.

For normalizing the C K-edge XAS spectrum, the first issue to be considered is the incorrect variation of raw XAS signal. These variations can be caused by many factors. Figure 3.14 shows a generalized schematic diagram of the XAS experiment at BL3.2a.The first issue to be considered is the background from the effect of the beamline, which causes the unwanted signal in the raw XAS signal (especially in C k-edge region). These variations background are from a number of factors, including the photon energy shift caused by electron beam fluctuations in the ring current or unwanted absorption signal from carbon contamination on the beamline optics (monochromator, grating, mirror etc.).Therefore, these backgrounds should be removed. Normally, the gold mesh is used to measure photon flux in front of the analysis chamber for background subtraction. This drain current is called the I_0 signal. In principle, the gold has no absorption in the C, N K-edge regions and a very small absorption in O K-edge region. The C K-edge signal from the gold mash has only the signal from background beamline. Thus, the background beamline in the raw signal can be subtracted by divided with I_0 signal.

Then background of beamline subtracted can be represented as

$$I_{sub} = \frac{I_{sample}}{I_0}, \tag{3.2}$$

where I_{sub} corresponds to the subtracted signal and I_{sample} correspond to the raw current signal from the sample. However, the gold mesh is commonly covered by unexpected carbon, e.g. carbon contamination in the beamline. As a result, the raw XAS signal is distorted. This distortion signal can be remedied by calibrating with the signal of form clean Au. This signal is called the I_{gold} signal. In theory, the raw data of clean Au or I_{gold} signal consists of two signals, the background of the beamline and unwanted signal from gold mesh contaminate. When I_{gold} signal is subtracted background by I_0 signal, the remaining part was showed only data of contaminants on the gold mesh. Hence, the all background in raw XAS signal can be removed by double background subtraction, the first is background from the beamline and the second one is background from the gold mesh. Where signal arise from double background subtraction was called $I_{double\ sub}$, Eq. (3.2) can then be revamped to:

$$I_{double\ sub} = \frac{\left(\frac{I_{sample}}{I_0}\right)}{\left(\frac{I_{gold}}{I_0}\right)} \quad (3.3)$$

In general, the synchrotron flux has not stable. It would gradually decrease over time. When measuring more than one sample, each measurement was spending a different time. The uses of synchrotron flux on each experiment are different too. The radiation beam angle that falls on the monochromator may change on each time leading to the photon energy shift from time to time. Therefore the signal taken at different times should be aligned photon energy before background removal. The difference in photon energy of I_0 between clean gold and DLC sample were shown fig 3.15. The photon energy calibration can be made by shifting the X-axis to coincident with the desired signal (all I signals should be shifted to the same position). In the last step, the signals were normalized to enable comparison with other spectra. Usually, the pre-edge of the spectrum was seated at 0 and the post-edge was defined to 1. The processing diagram of the XAS spectra is presented step by step below (Masrur, 2016) (Karen, 2011).

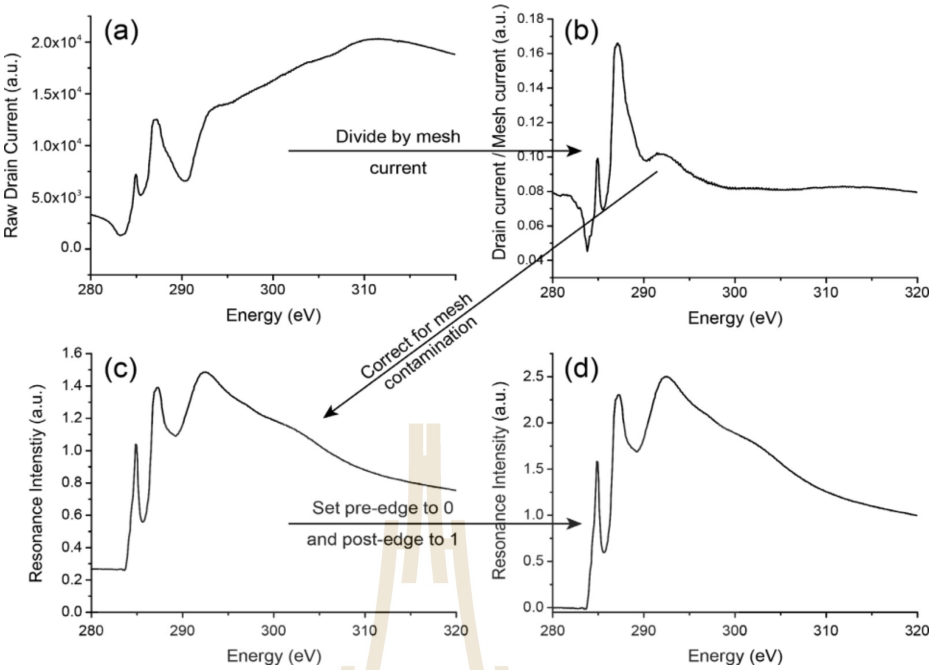

Figure 3.15 (a) Raw drain current spectrum. (b) the spectrum corrected by mesh current. (c) spectrum corrected for carbon contamination of the mesh. (d) spectrum with pre-edge (280 eV) set to 0 and post-edge (320 eV) set to 1 (Masrur, 2016).

CHAPTER IV

RESULTS AND DISCUSSIONS

This chapter presents the experimental results and discussion of the effect of surface contamination on XAS analysis of DLC films. The experiments were carried out at the BL3.2Ua beamline of the Synchrotron Light Research Institute (SLRI). Firstly, XPS analysis of surface contamination on DLC film is reported and discussed. Surface contamination on the optical elements of the synchrotron beamline is also mentioned. The amount of surface contamination on DLC film was controlled by an ion sputter cleaning technique. XAS spectra of the DLC films with different amounts of contamination were measured and analyzed. The results from the analysis were presented and discussed.

5.1 Unavoidable surface contamination on DLC films

In this work, DLC films were prepared by a HiPIMS technique. The films were deposited on glass substrates with dimensions of 2×2 cm^2 under the base and operating pressures of 2.7×10^{-5} and 2.2×10^{-2} mbar, respectively. Graphite with 99.99% purity was used as the target material. For deposition of DLC film, the deposition time was 60 minutes and the average power was 157 watts. Surface contaminations on the DLC films were characterized by means of X-ray photoelectron spectroscopy (XPS) because the technique is highly surface sensitive.

In the XPS measurements, soft X-ray with photons energies of 400 and 650 eV were employed for the excitation. The figure 4.1 represents typical XPS survey spectra taken from DLC films. The contributions from C 1s and O 1s and were clearly identified as the peaks at ~285 eV and ~531 eV, respectively. It is understable that the C 1s peak shall be observed from the measurements since the carbon is the composition of DLC. , The O 1s peak at 531 eV, however, indicates the existing of oxygen. The detected oxygen was identified as adsorbed oxygen on the film surface because the sample was exposed to air during transporting from the sample preparation system to the analysis system.

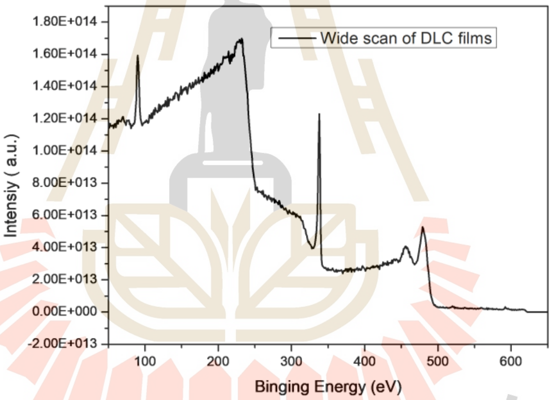

Figure 4.1 XPS survey scans spectra of the DLC sample.

The C1s and O1s XPS spectra taken from the DLC sample before and after ion sputter cleaning from different durations are shown in figure 4.2. It is well-known that a clean surface right after being brought out from a vacuum chamber can easily be contaminated from adsorption of air molecules. The surface of the sample was gradually cleaned to remove the contaminants by using 0.5eV Ar-ion sputtering. The reduction of the surface contamination is obvious as observed from the O1s and C1s

XPS spectra. The XPS results show that the C 1s peak tends to increase when the cleaning time increases, while oxygen peak significantly decreased. This is evidence showing that there are unavoidable contaminants on the surface of the sample and they are gradually removed by Ar-ion sputtering as the puttering time increases. Since XPS is a surface sensitive technique, the more surface contamination is removed, the more C1s signals from DLC are detected.

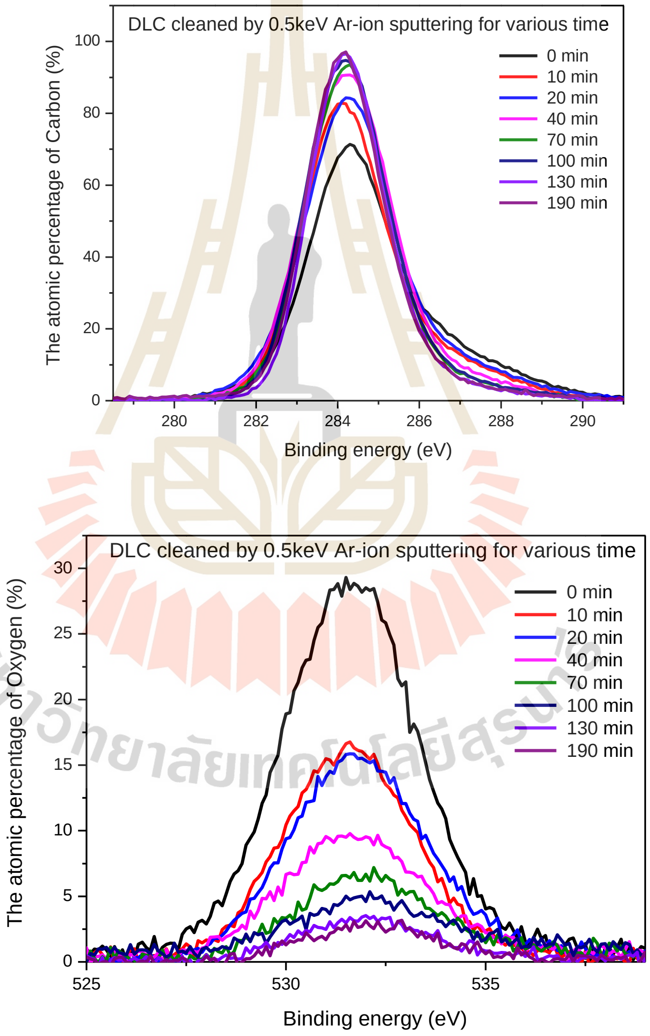

Figure 4.2 a) C1s XPS spectra and b) O1s XPS spectra taken from the DLC films before and after surface cleaning for various durations.

The atomic percentage of carbon and oxygen for the DLC sample before and after 0.5keV Ar-ion sputter cleaning for different durations are plotted in Figure 4.3. Oxygen of at 28.57% was found on the sample without cleaning. It is noted that the carbon percentage is contributed from both DLC and the contamination. With increasing the sputtering time, the amount of detected oxygen reduced. The oxygen content was difficult to remove to be below 3 at.% even with a prolong ion sputtering.

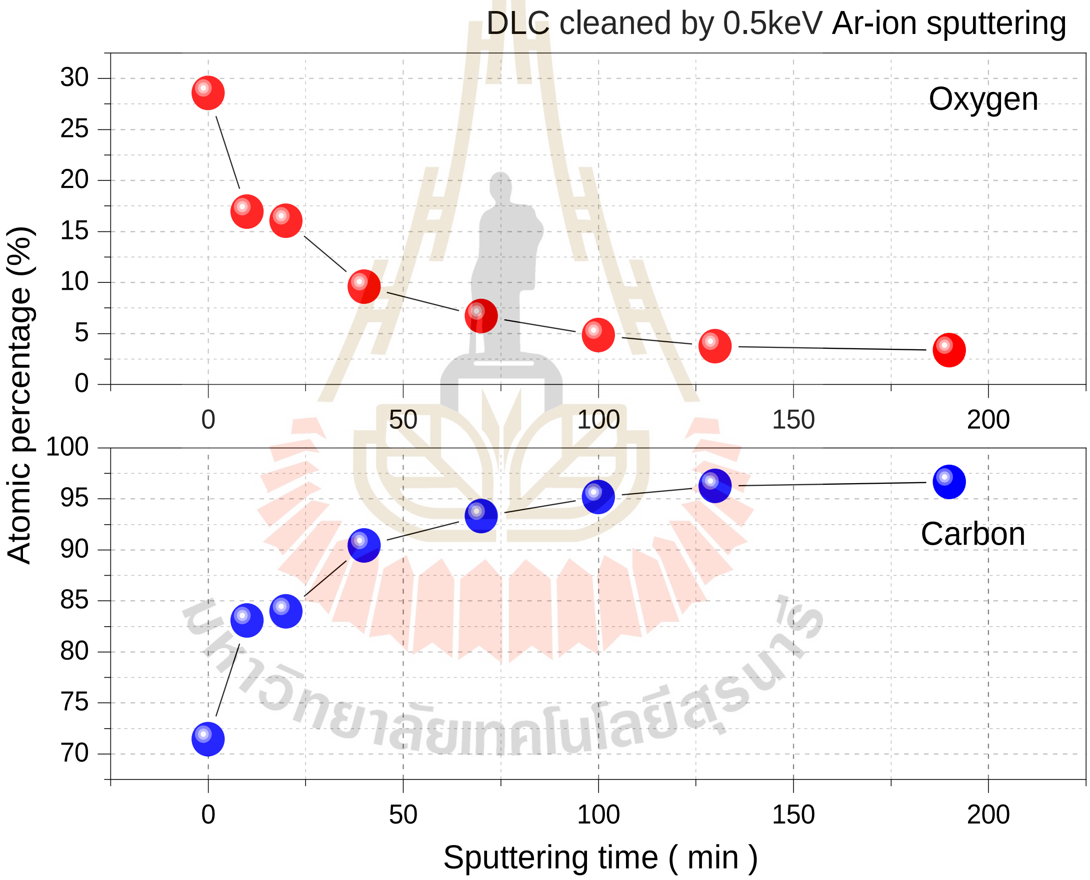

Figure 4.3 The Atomic percentage of carbon and oxygen in the DLC film sputtering of XPS

For detailed analysis of C1s XPS peak, different carbon species, such as sp^2 or sp^3 carbons, can be estimated by the deconvolution of C1s peak. The components of the whole C1s peak obtained from the deconvolution depend on the species of carbon or the structure that is assembled within the material. The deconvolutions of the XPS spectra were carried out using the Gaussian peak fittings. Figure 4.4 shows the C1s XPS peak taken from the DLC film before surface cleaning. The deconvolution of the spectra showed that the broad C 1s peak composes of four peaks with the peak positions at 284.5, 285.1, 286.8 and 288.4 eV. The small peaks at 283.5 is attributed from sp carbon. The assignments of the C1s peaks are given in table 4.2. The C1s peaks at 284.5 and 285.1 eV corresponds to the graphitic structure (the sp^2 carbon (C=C)) and the diamond structure (the sp^3 carbon (C-C)), respectively. Two more C species existing in the C1s XPS spectrum are attributed to carbons atoms with different bonding configurations, i.e. C-O, C=O and O-C=O. This result indicates that, in addition to oxygen, carbon also exists as the contaminations. Thus the C1s XPS peak originated from both DLC and surface contamination.

Table 4.2 Assignment of C1s XPS peaks taken from the DLC film.

Binding energy (eV)	**Peak Area (%)**	**Assignment**
283.5	5.83361	C≡C (sp)
284.5	62.80355	C=C (sp^2)
285.1	13.85687	C-C (sp^3)
286.8	10.4716	C-O
288.4	7.03437	C=O

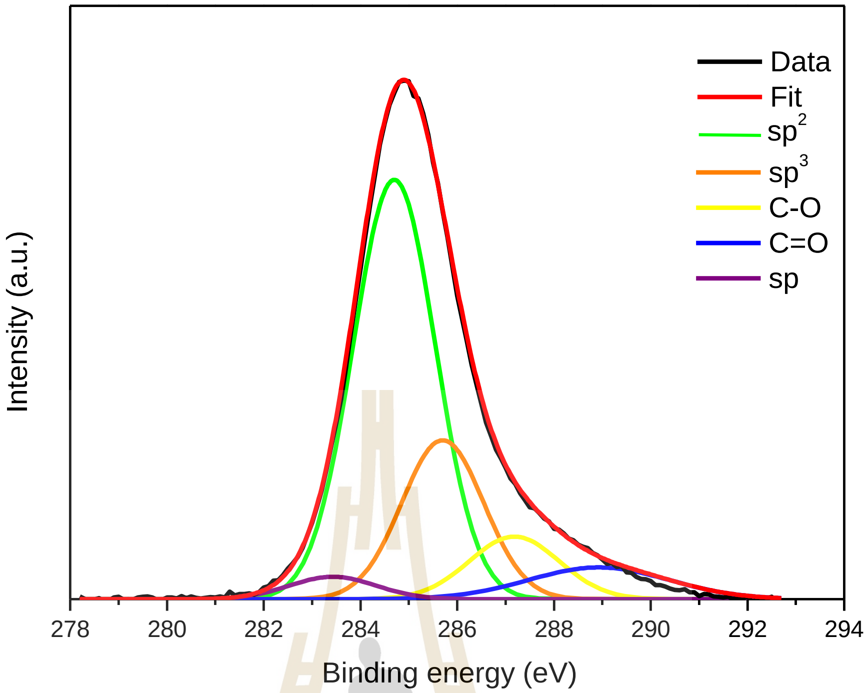

Figure 4.4 The fitting of C1s XPS spectra and b) The fitting of O1s XPS spectra.

Figure 4.5 shows the fitted percentages of carbon with different species obtained from the convolutions of C1s peak taken from the DLC sample before and after sputtering cleaning for various durations. Carbon species that are bonded with an oxygen atom are plotted by a filled circle symbol. These carbons might be regards as the surface contamination. The DLC film composes of sp^2 and sp^3 carbons, plotted by filled square and filled up-pointing triangle symbols, respectively. The filled down-pointing triangle symbol represents the summation of sp^2 and sp^3 carbons, i.e. DLC. The detected surface contamination of about 26.54% is on the surface of the DLC film before the sample was surface cleaned by ion sputtering. The contamination decreases with increasing sputtering time until about 100 min sputtering time. After that, there is no significant reduction of the surface contamination. The reduction of the surface contamination allows more C1s photoelectrons from DLC (sp^2 + sp^3) to escape from the sample and be detected by the electron energy analyzer of the XPS system. It is interesting to point out that, from the XPS results, the surface contamination could not be eliminated by 0.5keV Ar-ion sputtering. The contamination of about 6.22% remains on the surface even though prolong sputtering was carried out. There might be the possibility that carbons bonded with oxygen might not be on the surface but in the films. This issue was clarified by more experiments with the results and discussion given below.

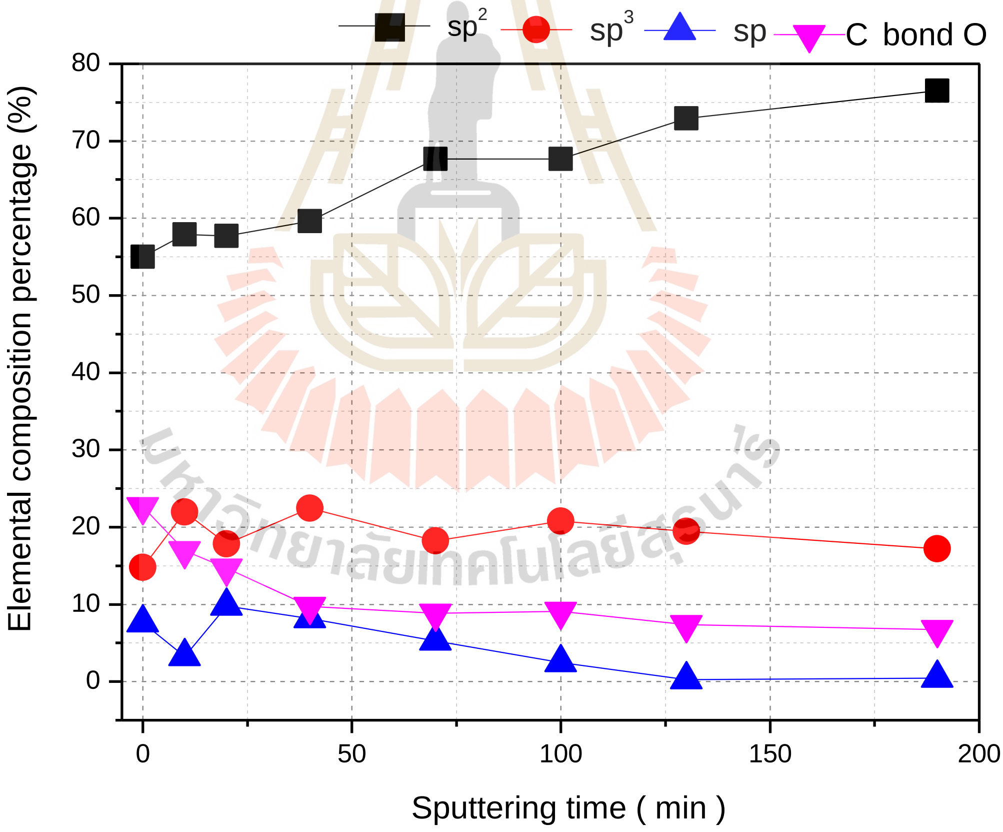

Figure 4.5 Percentage of different carbon species in the DLC film before and after sputtering cleaning for various durations at photon energy 650 eV.

It is interest also to point out the variation on the composition of the sp^2 and sp^3 carbons in the DLC films with the sputtering time. This indicates the change in sp^2 and sp^3 ratio with the changes of the probed depth of the XPS measurement technique. The origin of this variation is complicated. It might be due to either the effect of ion induced effect or the deposition conditions. This problem was not tackled in this thesis work.

As mentioned above, carbon species that are considered as the contamination cannot be eliminated by 0.5keV Ar-ion sputtering. This raises the question that the remaining oxygen might also in the film. Therefore, more XPS measurements were carried out on the DLC films clean by using higher energy of Ar-ion for sputtering. These measurements were performed in a stand-alone XPS system with Al Kα as the excitation. It is clearly observed that the amount of the remain oxygen decrease with increasing AR-ion energy, as shown in figure 4.6. This indicates that the oxygen is mainly from the surface contamination.

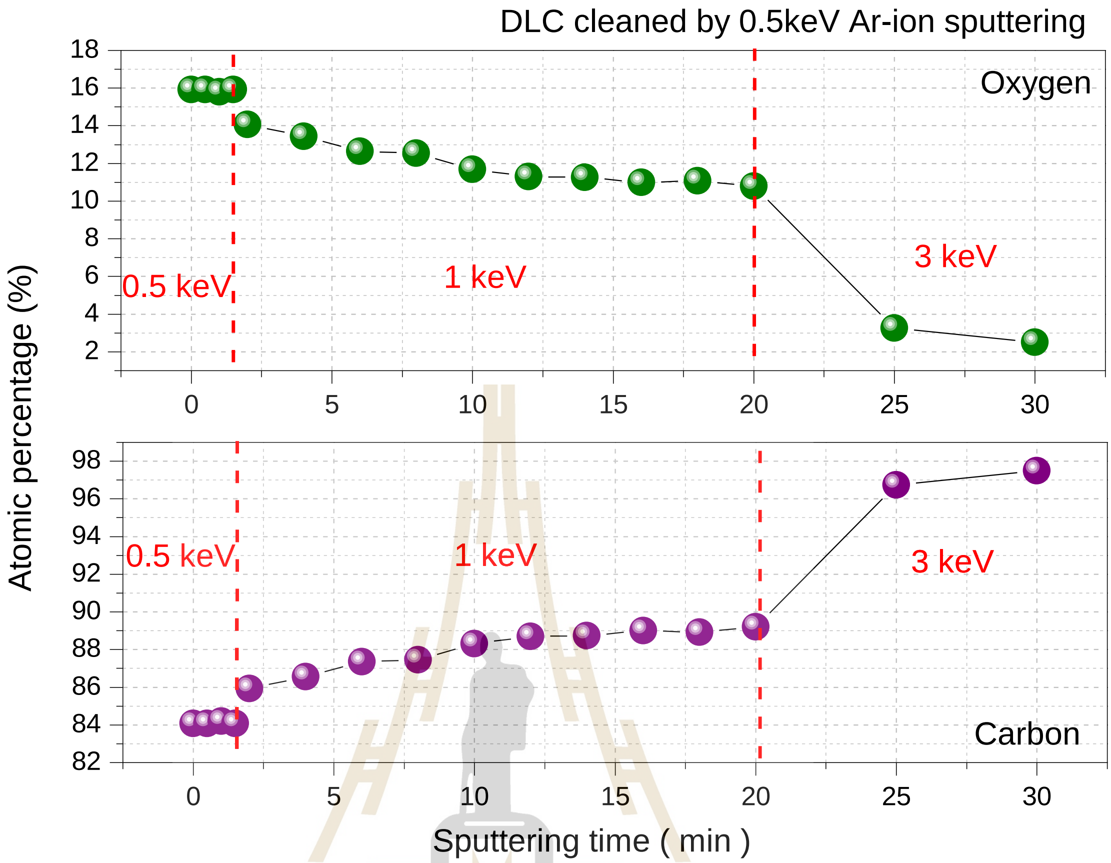

Figure 4.6 The Atomic percentage of carbon and oxygen in the DLC film sputtering of XPS at BL 5.2.

5.2 Contamination on optical elements of a synchrotron beamline

This section covers the study of contamination on optical elements of synchrotron beamlines. In electron-yield mode of XAS measurements, gold mesh with high purity is used for measuring an incoming photon flux just in front of the sample. The drained current from the gold mesh is used for normalization of the absorption spectra. For measuring C K-edge XAS spectra, the drain current includes the information of carbon contamination on the gold mesh resulting in the incorrect value of the incident photon current. Thus, the correction was made with the procedures described below, and more details are mentioned in Chapter III. The correction of an C K-edge XAS spectrum of any sample caused by the incorrected incident photon current can be done by normalization of the spectrum with the C K-edge spectrum measured from a cleaned gold sample. This is illustrated below

Figure 4.7 Shows C1s and Au 4f XPS spectra taken from a 99.99%-pure gold sample before and after cleaning. The present of carbon indicates that there is contamination of the surface of the gold sample. The contamination was removed by 0.5keV Ar-ion sputtering. As expected, after the surface contamination is eliminated, more photoelectrons from the gold sample could escape and be detected resulting in the increase of the Au 4f peak, as shown in the figure.

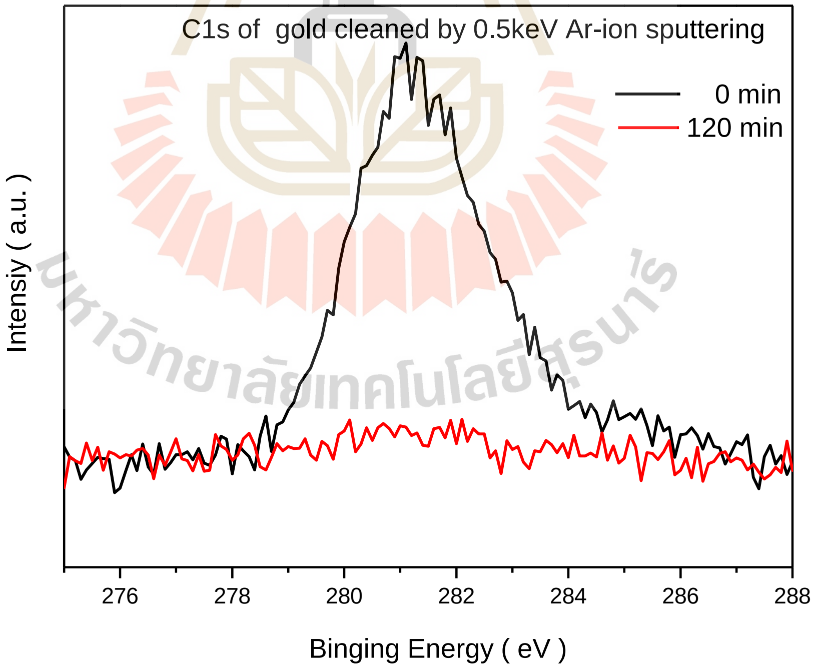

Figurg 4.7 C1s XPS spectra on pure gold, b) Au4f XPS spectra on pure gold before and after cleaned surface.

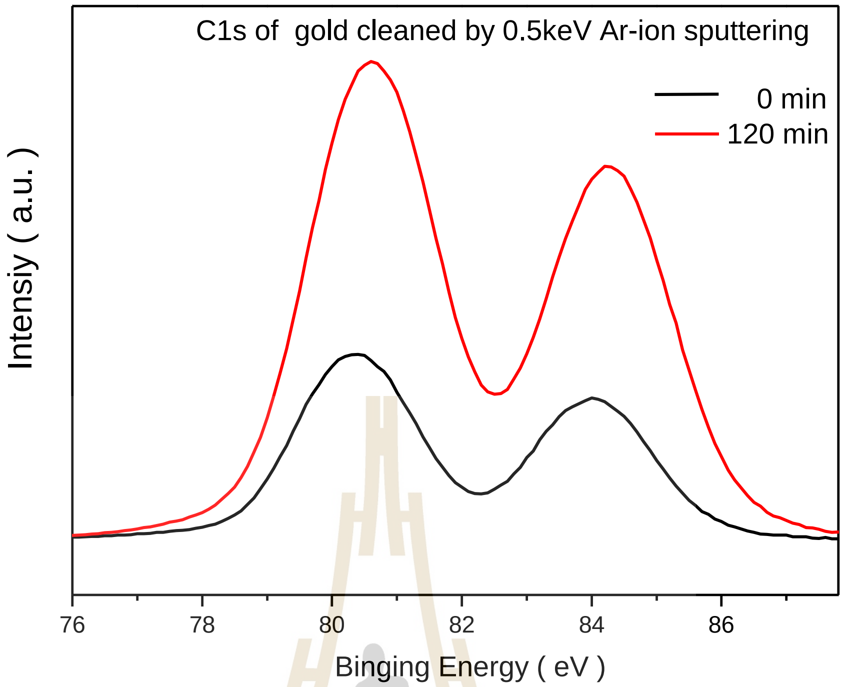

Figurg 4.7 C1s XPS spectra on pure gold, b) Au4f XPS spectra on pure gold before and after cleaned surface (Continued).

In a total electron-yield mode of XAS measurement, the absorption spectrum is given by;

Absorption spectrum of a sample $=> \left(\frac{I_{sample}}{I_{0\_sample}}\right)$

where I_{sample} is the drain current of the sample, and I_{o_sample} is the drain current of the gold mesh. To remove the effect of the incorrected drain current of the gold mesh caused by the present of the contamination on the gold mesh, the C K-edge absorption spectrum of a cleaned gold is measured, which is;

Absorption spectrum of a cleaned gold $=> \left(\frac{I_{gold}}{I_{0\_gold}}\right)$

Where I_{gold} is the drain current of the cleaned gold sample, and I_{o_gold} is the drain current of the gold mesh. To remove the effect of the contamination on the gold mesh, the absorption spectrum of the sample is normalized with the spectrum of the clean gold, as the following

$$\text{Corrected absorption spectrum of a sample} => \frac{\left(\dfrac{I_{sample}}{I_{0\_sample}}\right)}{\left(\dfrac{I_{gold}}{I_{0\_gold}}\right)}$$

C K-edge absorption spectra of gold before and after surface cleaning are shown in Figure 4.8. There are absorption features on both spectra. The existing of the C K-edge absorption feature on the gold sample without cleaning is not surprised. However, after the carbon contaminant is remove, the absorption feature remains. This is due to the fact that there is absorption by carbon on the gold mesh. This absorption spectrum of the clean gold sample is used to normalize C K-edge absorption spectra of different samples. The C K-edge absorption spectra of a DLC sample with and without correction by the spectrum of a cleaned gold sample are shown in figure 4.8. The two spectra show noticeable differences. The noticeable changes occurred in features between 284.7-285.3 eV. This range corresponding to the $\pi*$ bands at 284.8 eV that is typical for the C=C bond (sp^2). This range is especially important in calculating the amount of sp2 content in the DLC films. Thus, It is possible about the dramatic change these ranges may have a relatively high impact on the DLC films analysis. Due to XAS spectrum in this region is used to estimate the sp^2 content in the DLC films, this infinitesimal change is important for calculating the sp^2 content.

This change caused a slight change in the normalize signal, shown in Figure 4.8.

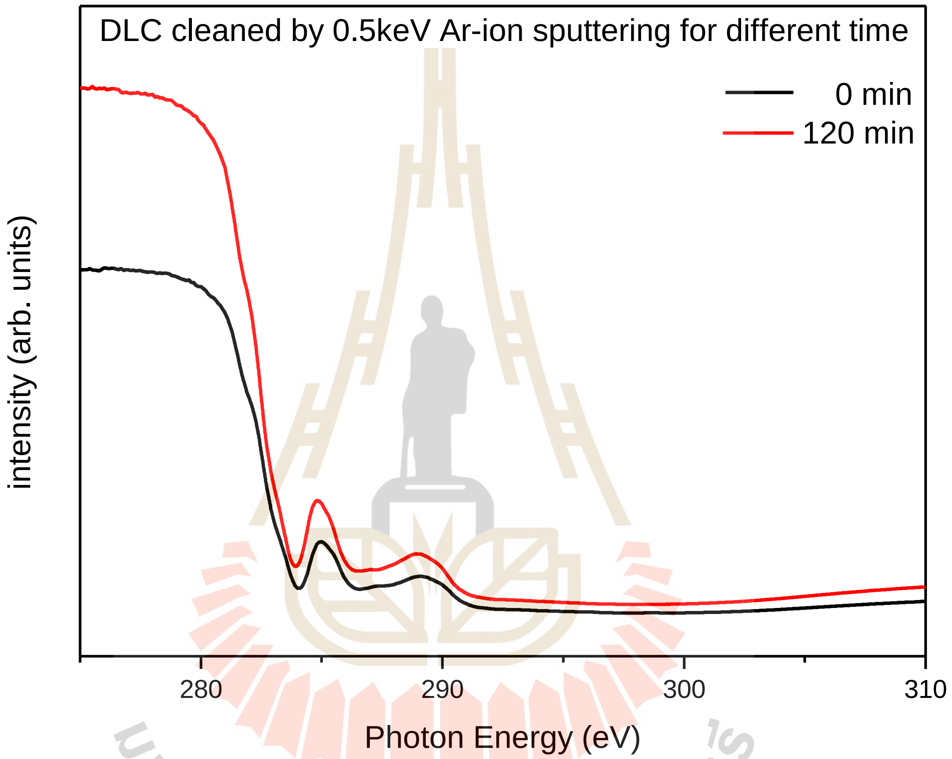

Figure 4.8 C k-edge XAS spectra on pure gold before and after cleaned surface.

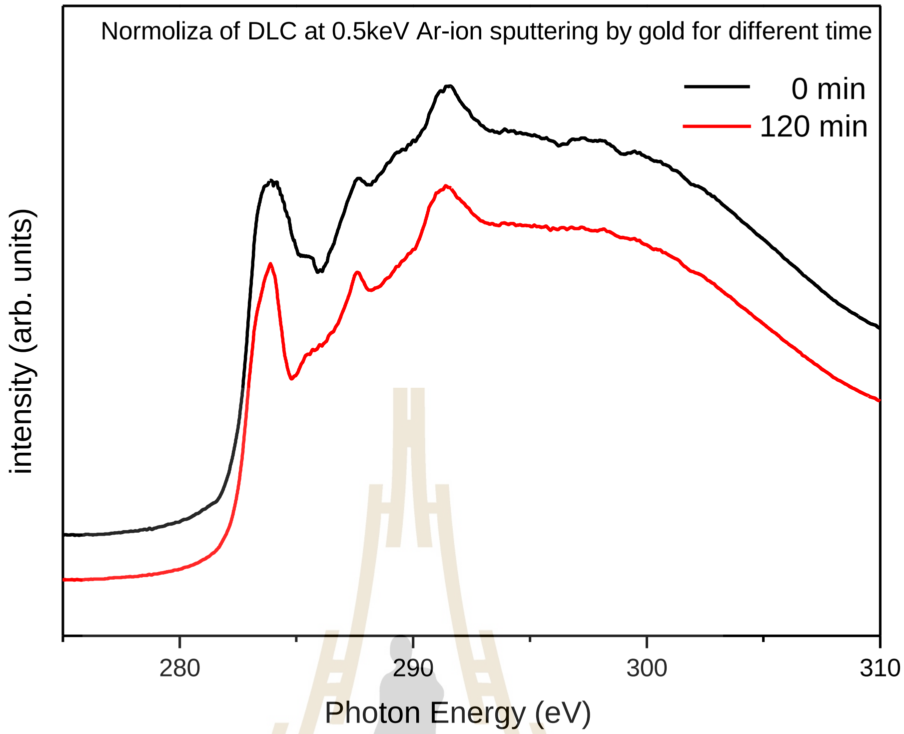

Figure 4.8 C k-edge XAS spectra on pure gold before and after cleaned surface (Continued).

5.3 XAS analyses of DLC

In the previous section, it has been demonstrated that how correct C K-edge absorption could be obtained. This section describes two different approaches to analyze C K-edge XANES spectra taken from DLC. The first one is the classical two-window method and the other is the fitting methods.

Figure 4.9 shows C k-edge XAS spectra taken from the DLC sample before and after sputtering cleaning for different durations. It is noted that all spectra have been corrected to remove the effect of the carbon contamination on the gold mesh, as described above. Surface cleaning was done by 0.5keV Ar-ion sputtering. After sputtering, the sample was measured by XPS technique to quantify the surface contamination and then follow by the XAS technique. It is obvious that there are some differences in the features between the XENES spectrum of the DLC sample before and after cleaning by ion sputtering. The features in the range of 284.8-285.3 eV and 288-292 eV are from graphite bonding (C=C) and the bonding between carbon and oxygen (C=O), respectively.

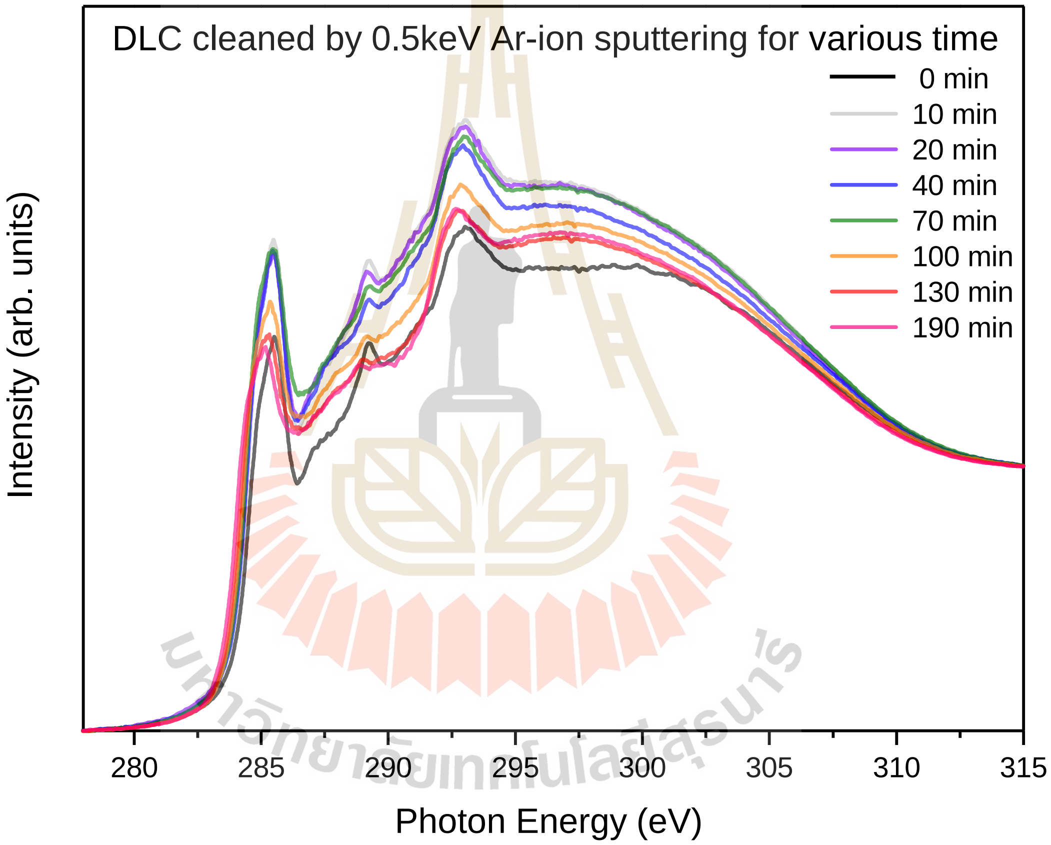

Figure 4.9 C k-edge XAS spectra on the DLC films before-after cleaned llsurface at different time.

5.3.1 Two-window methods

The pure graphite consists of 100% of the sp^2 hybridized carbon. Amorphous carbon and DLC contain a fraction of the sp^2 hybridized carbon. The fraction or percentage of the sp^2 carbon in amorphous carbon or in DLC can be estimated by comparing the $1\pi^*$ fraction with that of a pure graphite sample. The formula for the calculation is the following;

$$sp^2\ \% = \left(\frac{I_{\pi^*}}{I_{\Delta E}}\right)_{unknown} \Big/ \left(\frac{I_{\pi^*}}{I_{\Delta E}}\right)_{reference} \qquad (4.1)$$

where $I_{\pi*}$ is the integral of the $1s \rightarrow \pi^*$ transition and $I_{\Delta E}$ is the integrated counts for the normalizing energy window. The superscripts unknown and reference denote the standard and unknown spectra, respectively. Normally, as in this work, the reference sample is highly oriented pyrolytic graphite (HOPG). Figure 4.9 shows C K-edge XANES spectra of the DLC and HOPG reference samples. The percentage of the sp^2 carbon in the DLC samples before and after cleaning by ion sputtering for different durations were calculated and the results are shown figure 30.

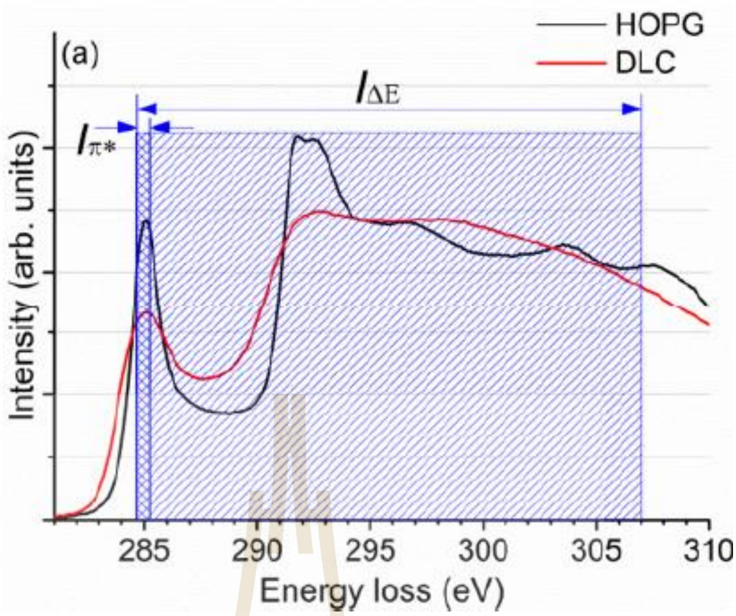

Figure 29 Schemes of sp^2-C quantification of DLC by referring to HOPG.

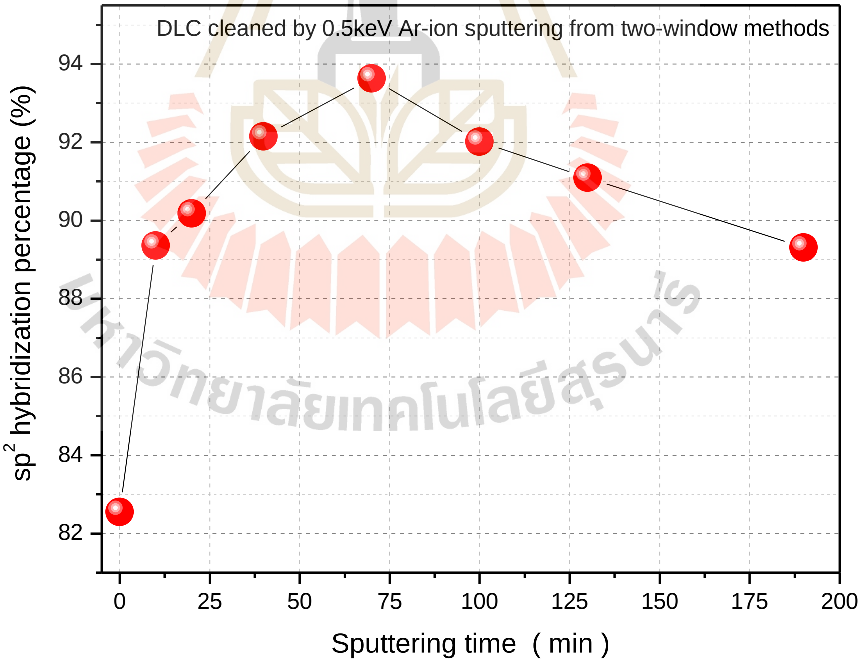

Figure 4.10 the percent of sp^2 of XAS spectra in cleaned surface at different ltime.

In figure 4.10, it is clearly seen that the sp^2 carbon is minimum for the DLC before cleaning by ion sputtering. The lowest percentage of the sp2 carbon is found for the case of the un-cleaned DLC sample. This indicates that the contaminating carbon on the surface of the DLC sample contributes to the C K-edge XANES spectrum resulting in a low estimated percentage of the sp^2 carbon, which is in the DLC films. A 10min ion sputtering results in a reduction of the surface contamination by nearly half, as shown in the O 1s XPS results in figures 4.2b and 4.3. There is a clear correlation between the reduction of the contamination and the increase in the percentage of the detected sp^2 carbon in the DLC film cleaned for 10min. It is understood that when the amount of the over layer of the contamination reduces, more signals from the DLC beneath are detected. The percentage of the sp^2 carbon increases with increasing the sputtering time, or with the decrease of the surface contamination. This increase continues up till the sputtering time of 70min. Then the sp^2 carbon content begins to drop, and keep decreasing with the sputtering time. The decrease of the sp^2 carbon with sputtering time might be due to the fact that ion sputtering might induce damage to the graphite structure. The results presented in figure 30 indicate that the surface contamination on DLC films affects XANES analysis of the sp^2 carbon fraction. Ion sputtering on DLC might also lead to damage of the structure of graphite.

It is note that, even though the estimation of sp^2 content by this method is widely accepted, it can only provide information of only the sp2 fraction. For DLC, sp^2 fraction must be estimated as well. Different approach for estimating the different carbon species simultaneously is described in the next section.

5.3.2 Deconvolution of XANES spectra

Base on the knowledge that a XANES spectrum composed of the different transition peaks and ionization function. Different peaks represent different carbon species. The percentage of the carbon species can be determined from the deconvoluted peak areas. The advantage of this method is that different carbon species, such as sp^2 and sp^3, can be obtained simultaneously.

Figure 4.11 shows an example of the convoluted C K-edge XANES spectrum taken from the DLC sample after cleaning by 0.5KeV Ar-ion sputtering for 0 min. The measured spectrum was deconvoluted by curve fitting, giving the Gaussian transition peaks (from 1s to the allowed orbitals) and the ionization step function [9]. The assignments of the obtained fitted peaks are given in table 2. The peaks corresponding to the $\pi\ast$ and $\sigma\ast$ bands at 284.8 eV and 292.2 eV are typical for the C=C bond (sp^2) and the tetrahedral C–C bond (sp3), respectively [10]. Other peaks are originated from different carbon species: Ketone/Aldehyde ($\sigma\ast$ C - H) at 286.7eV, carboxyl carbon (C = O(OH)) at 288.7 eV, Cls $\sigma\ast$ of C-C at 293.5 eV, Cls $\sigma\ast$ of C=C at 300eV and C1s $\sigma 1\ast$ of O=C-OH at 296.6 and C1s $\sigma 2\ast$ of O=C-OH at 303.5 eV [11,12].

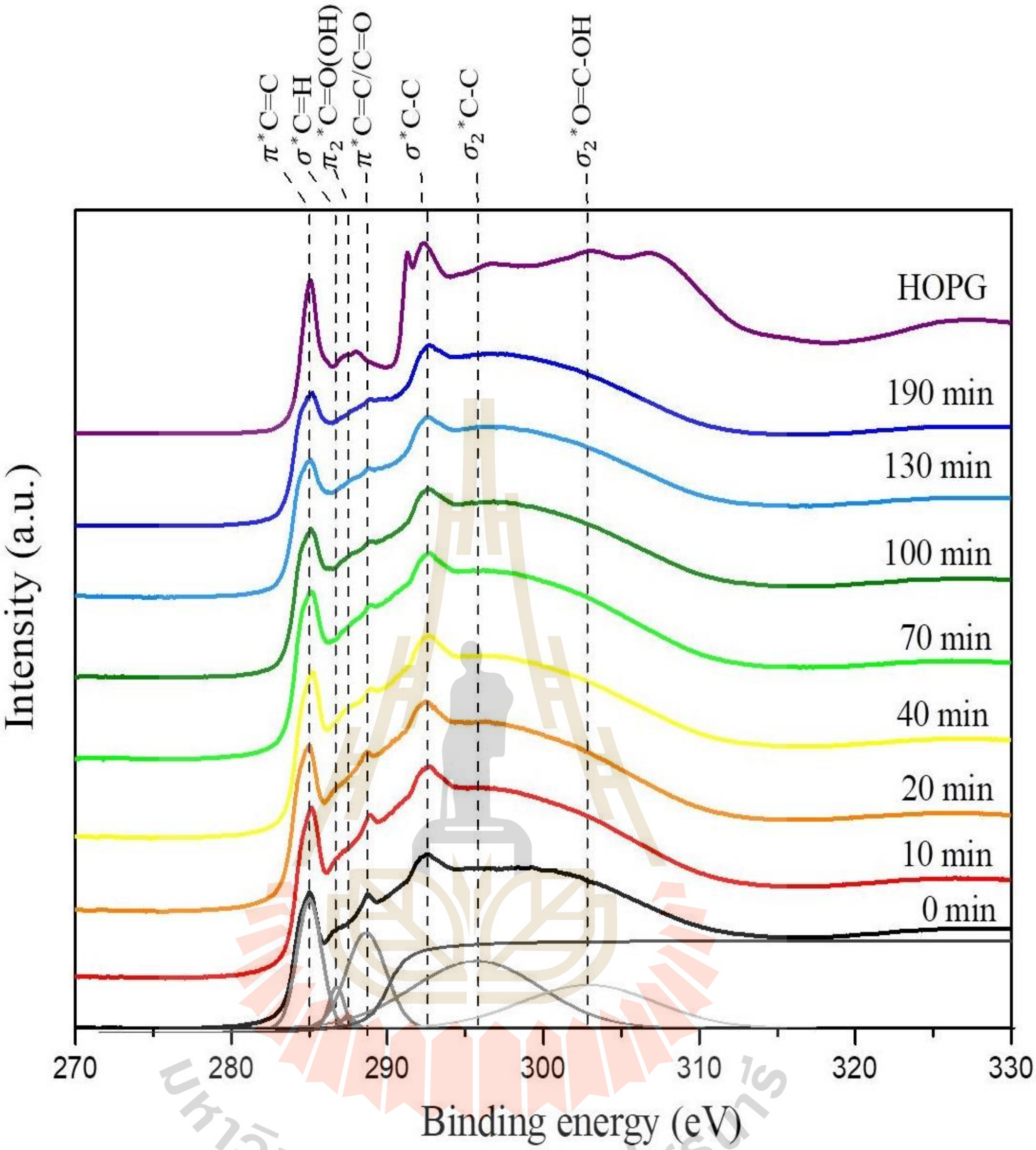

Figure 4.11 Normalized C K-edge XANES spectrum of DLC films with curve fitting.

Table 2 Peak assignment of the transitions from the 1s to different orbitals and the ionization energy.

Photon energy (eV)	**Peak Area (%)**	**Assignment**
285.2	6.65836	π^* C=C
286.1	12.1468	σ^* C-H
287.1	0.63447	π_2^* C=O(OH)
289	16.45233	π^* C=C/C=O
290	-	Ionization threshold
292.9	9.44127	σ^* C–C
296.3	22.73792	σ_2^* C-C
302.7	31.92886	σ^* O=C-OH

Figure 4.12 shows the sp^2 content deduced from the convolution of the XANES spectra taken from the DLC sample before and after cleaning by ion sputtering for different durations. In general, there are differences in the percentage the sp^2 carbon obtain from the two different approaches. However, the trend of the sp^2 fraction is similar. The lowest sp^2 content is observed for the DLC without cleaning. The maximum percentage sp2 content was found to be about 88 at. % after the surface of the DLC was sputtered by 0.5keV Ar-ion for 70 min. For the longer durations of sputtering, the sp^2 content was found to decrease.

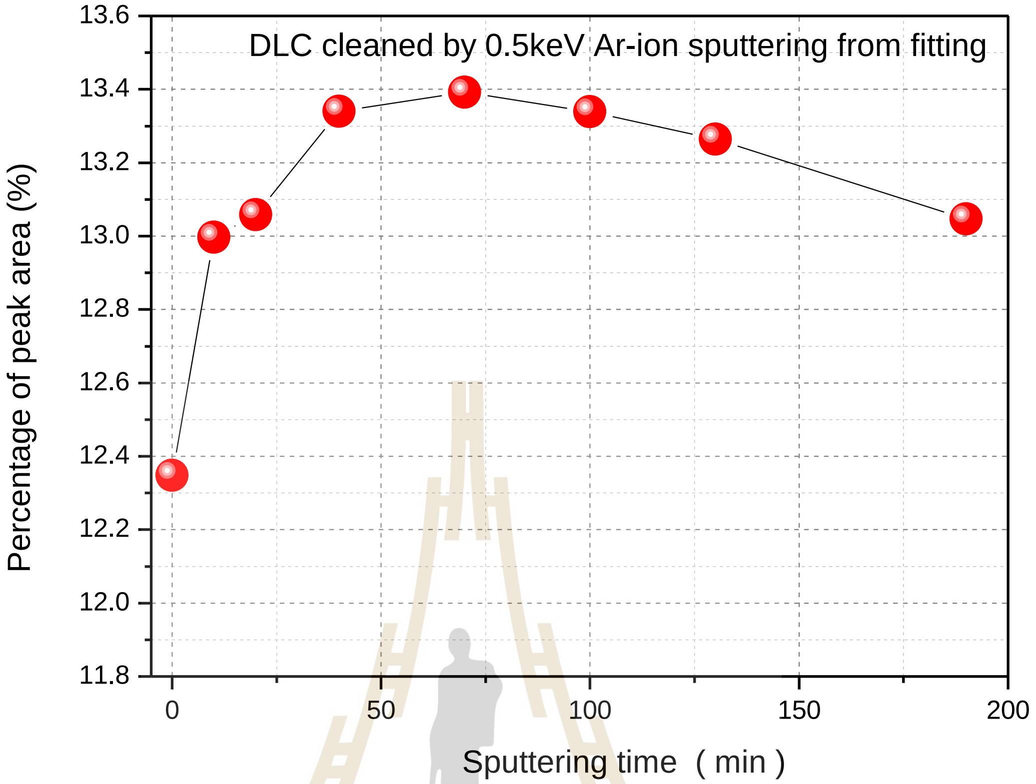

Figure 4.13 Percentage of sp^2 content deduced from the deconvolution of the C K-edge XANES spectra of DLC before and after cleaning by sputtering for various durations.

As mentioned above, the deconvolution approach provides more information of the analyzed sample. The peak area of π_2^* C=O(OH) can be used for estimating the carbon atoms bonded to oxygen. The percentage of those carbon atoms for the DLC sample before and after cleaning is shown in figure 4.14. It is shown by the XPS measurements, those oxygen atoms exist as contamination on the surface of the DLC film. It is obvious in the figure that 10min 0.5keV Ar-ion sputtering greatly reduces those contaminating carbon atoms, from 12 to 13 at. %.

The results from the two approaches for determining the sp^2 contents in DLC indicate that surface cleaning of the DLC films is required to get an accurate value of the sp^2 content in the film. Surface cleaning by low-energy ion sputtering could remove the contaminating toms such as oxygen and carbon. The present of the contaminating carbon leads to wrong values of the carbon content in the film. Prolong sputtering might also cause the damage to the sp^2 bonds.

CHAPTER V

CONCLUSIONS AND REMARKS

This thesis demonstrates that the DLC films contain contamination of the surface after taking them out from the preparation chamber and exposing to air. The main contaminating elements are carbon and oxygen. The surface contamination originated from the adsorption of air molecules on the surface of the DLC films.

It is very unfortunate when the element of the sample to be analyzed is the same element as the contaminating element. For the case of DLC, carbon in the thin film and surface contaminating carbon cannot be distinguished by certain analytical techniques. In this work, chemical sensitive technique such as XPS and XAS were employed to distinguish carbon species. For XAS, the technique requires a continuous and board spectral synchrotron light. To utilize the synchrotron light to produce XAS spectra, an incident photon current/flux before hitting on the sample is used for the normalization. The photocurrent is normally measured by a gold mesh. It has well known and also shown in this work that the wires of the gold mesh are also cover with contaminating carbon that lead to obtain incorrected C K-edge XAS spectra. However, the effect of the contamination on the gold mesh can be removed with normalization of a C K-edge XAS spectrum of a cleaned gold sample.

Two different approaches have been employing to analyze the absorption spectra. It was found that surface contamination on the DLC films lead to the lower values of the sp3 and sp3 carbon in the DLC films. This is due to that fact that the signals form the surface contamination is also collected during measuring the absorption spectra. The carbon species of the contamination are different from those in the DLC films. Thus to obtain accurate percentage of the carbon species in the DLC films, in-situ surface cleaning techniques such as low-energy Ar-ion sputtering is necessary. However, sputtering may cause the damage to the film material as well. Thus, sputtering time and power must be properly chosen to avoid the damage to the DLC. In this work, it was found that 70min sputtering time is optimum for 0.5keV Ar ions.

REFERENCES

REFERENCES

ANSTO group. (1987). **How is synchrotron light created** [on-line]. Available: https://www.ansto.gov.au/education/nuclear-facts/what-is-synchrotron-light.

Blackmore, P.D., Birtwhistle, D. (2004). Evaluation of cross-linking after accelerated photoageing of silicone rubber, **Polymer International**. 53: 163-168.

Biesinger, M.C. (2018). **Depth of Analysis, Inelastic Mean Free Path** (on-line). Available: http://www.xpsfitting.com/2012/08/depth-of-analysis-inelastic mea free.html.

Briggs, D., and Seah, M.P. (1990). Practical surface analysis: Vol. 1 - Auger and X-ray photoelectron spectroscopy, 2nd ed. John Wiley & Sons, Fabien.

Christie, A.B. (1989) "X-ray photoelectron spectroscopy," in Methods of surface analysis: Techniques and applications. Cambridge University press.

David, B., Florence, DJ., Mohamed, B., and Jacques, L. (2004). Evaluation of cross-linking after accelerated photoageing of silicone rubber, **Polymer International**. 53: 163-168.

Georg, H. (2006). Near edge X-ray absorption fine structure spectroscopy as a tool to probe electronic and structural properties of thin organic films and liquids. **Chemical, Soc, Rev.** 35: p. 1244.

Helmersson, U., Lattemann, M., Bohlmark, J., Ehiasarian, A.P., and Gudmundsson, J. T. (2006) Ionized physical vapor deposition (ipvd). A review of technology and applications. **Thin Solid Films.** 513(1-2): 1-24

Lenhart, J.L., Fischer, D.A., Sambasivan, S., Lin, E.K., Jones, R.L., Soles, C.L., Wu, W., Goldfarb, D.L., and Angelopoulos, M. (2005). X-ray Absorption Spectroscopy to Probe Surface Composition and Surface Deprotection in Photoresist Films. **Langmuir**. 21(9): 4007-4015.

Meidong, H., Xueqian, Z., Peiling, K., and Aiying, W. (2013). Graphite-like carbon films by high power impulse magnetron sputtering. **Appl. Surf. Sci.** 283: 321-326 Merel, P., Tabbal, M., Chaker, M., Moisa, S., and Margot, J. (1998). Direct evaluation.

Merel, P., Tabbal, M., Chaker, M., Moisa, S., and Margot, J.(1998). Direct evaluation of the sp3 content in diamond-like-carbon films by XPS. **Appl. Surf. Sci** 1 36(1-2): 105-110.

Mohai, M. (2000). The mean free path [on-line]. Available: http:// www .lasurface. com/xps/imfp.php.

Ozlem Duyar Coskun and Taner Zerrin. (2013). Properties of ITO–AZO bilayer thin films prepared by magnetron sputtering for applications in thin-film silicon solar cells. **Diamond Relat. Mater.** 110(1): 41-45.

Quiros, C., Soriano, L., Gomez, J.G., Palomares, F.J., Elizalde, E., Bressler, P.R., and Sanz,J.M. (1999). XAS and XPS study of amorphous carbon nitride films. **Bessy Jahresbericht 1999. (Annual report 1999 of the Berliner Elektronenspeicherring-Gesellschaft fuer Synchrotron strahlung (BESSY)).**

Paul, B., Simon, J., and Martin, V. (2006). **Properties of Synchrotron Radiation** [on-line]. Available: http://pd.chem.ucl.ac.uk/pdnn/inst2/prop.htm.

Rajkumar, D., Sukdev, D., Shamima, H., Radhaballav, B., and K.P. Arun. (2018). Phosphorus doping of diamond-like carbon films by radio frequency CVD-cum-evaporation technique. **Diamond Relat. Mater.** 82: 70-78.

Robertson, J. (1992). Mechanical Properties and Coordinations of Amorphous Carbons**. Phys. Rev. Lett.** 68(2): 220-223.

Raúl, B. (2000). **Electron-surface interactions** [on-line]. Available: https://www2. Virginia.edu/ep/SurfaceScience/electron_interactions.htm.

Shin-ichi, H., Ryosuke, T., Yusuke, N., Akira, T., Masahito, N., Mititaka, T., Ryuji, H., Hirokazu, I., Hideki, Y., Keisuke, N., Eiji, T., Kuei-Yi, L., and Masaki, O. (2014). Transformation of multiwalled carbon nanotubes to amorphous carbon nanorods under ion irradiation. **Japan J Appl Phys.** 53(2S): 02BD06.

Shinya, O., Tsuyoshi, Y., Akira, N., Sausan, AL-R., Ryota, O., Hiroyuki, S., Eiichi, K., and Kunihito, N. (2009). Near-Edge X-Ray Absorption Fine Structure of Ultrananocrystalline Diamond/Hydrogenated Amorphous Carbon Films Prepared by Pulsed Laser Deposition. **J. Nanomater.** 876561: 5.

Sainio, S., Nordlund, D., Caro, M.A., Gandhiraman, R., Koehne, J., Wester, N., Koskinen, J., Meyyappan, M., and Laurila, T. (2016). Correlation between sp3-to-sp2 Ratio and Surface Oxygen Functionalities in Tetrahedral Amorphous Carbon (ta-C) Thin Film Electrodes and Implications of Their Electrochemical Properties. **J. Phys. Chem. C**. 120(15): 8298-8304.

Steinberger, R., Celedón, C.E., Bruckner, B., Roth, D., Duchoslav, J., Arndt, M., Kurnsteiner, P., Steck, T., Faderl, J.,. Riener, C.K., Angeli, G., and Bauer, P. (2017). Oxygen accumulation on metal surfaces investigated by XPS, AES and LEIS, an issue for sputter depth profiling under UHV conditions. **Appl. Surf. Sci.** 411: 189-196**.**

Stöhr, J. (1992). NEXAFS Spectroscopy. Springer Series in Surface Science. Springer Verlag, Berlin. Vol. 25.

Tony, B., and David, B. (2005). Electrical properties of polymers, 2nd ed. Cambridge University Press.

Tsukagoshi, A., Honda, S., Osugi, R., Okada, H., Niibe, M., Terasawa, M., Hirase, R., Izumi,H., Yoshioka, H., Niwase, K., Taguchi, E., Lee, K.Y., and Oura, M. (2013). Spectroscopic characterization of ion-irradiated multi-layer graphenes .**Nucl. Instrum. Methods B**. 315: 64-67.

Vickerman, J.C., and GilmoreI, S. (1997). Surface Analysis - The Principal Techniques,Wiley, Chichester.

Wilson, E.J.N. (1996). "Fifty Years of Synchrotrons". CERN, Geneva, Switzerland. **Conference proceeding**.

Yael, I., Jacques, L., Jacques, C., and Jacques, L. (1993). Photo-oxidation of polydimethylsiloxane oils: Part III - Effect of dimethylene groups, **Polym Degrad Stabil**. 42: 267-279.

Yasuji, M.,Satoshi, U., and Eric, M. (2009). Quantitative and chemical-state analyses of surface oxygen on graphite oxides using total-electron-yield soft X-ray absorption spectroscopy. **Carbon**. 47(5): 1412.

Yukimura, K., Konishi, T., Takaki, K., and Nakao, S. (2015). Fabrication of diamond-like carbon films using short-pulse HiPIMS. **Surf. Coat. Technol.** 286: 239-245.

Zemek, J., Jiricek, P., Houdkova, J., Artemenko, A., and Jelinek, M. (2016). Diamond-like carbon and nanocrystalline diamond film surfaces sputtered by argon cluster ion beams**. Diamond Relat. Mater.** 68: 37-40.

APPENDIX

APPENDIX

LIST OF PUBLICATION

Lomon, J., Chaiyabin, P., Saisopa, T., Seawsakul, K., Saowiang, N., Promsakha, K., Poolcharuansin, P., Pasaja, N., Chingsungnoen, A., Supruangnet, R., Chanlek, N., Nakajima, H., and Songsiririthigul, P. (2018). XPS and XAS preliminary studies of diamond-like carbon films prepared by HiPIMS technique. **Journal of Physics: Conference Series**.

Chaiyabin, P., Giboni, K.L., Han, K., Ji, X., Juyal, P., Kobdaj, C., Liu, J., Lomon, J., Pasaja, N., Poolcharuansin, P., Rujirawat, S., Songsiririthigul, P., Yan, Y., and Zhao, L. (2017). Novel field cage design for the PandaX III double beta decay experiment. **Journal of Instrumentation**.

CURRICULUM VITAE

Name : Miss Jidapa Lomon

Nationality : Thai

Date of Birth : 15 April 1994

Address : 55 Mu.4, T. Phangdang, Thatphan
District, Nakhon Phanom, 48110
Thailand
Tel. +66-64-9487171

E-mail : dreemda55@gmail.com

Education Background :

2012-2016 B.Sc. (Physics) Ubon ratchathani university, Ubon ratchathani, Thailand.

2016-2019 M.sc. (Physics) Suranaree University of Technology with Scholarship, Nakorn Ratchasima, Thailand.

Work Experience :

1. M.sc. Research under PandaX collaboration at shanghai jiao tong university, Shanghai, China.
2. M.sc. Student Research Assistant at Photoemission beamline BL5.3 at Synchrotron Light Research Institute (Public Organization), Thailand.
3. Teaching Assistant at Laboratory, School of Physics, Suranaree University of Technology, Thailand.